AD_____

Award Number DAMD17-96-1-6029

TITLE: Immunobiological Aspects of erbB Receptors in Breast Cancer

PRINCIPAL INVESTIGATOR: Mark I. Greene, M.D., Ph.D.

CONTRACTING ORGANIZATION: University of Pennsylvania
Philadelphia, Pennsylvania 19104-3246

REPORT DATE: August 1999

TYPE OF REPORT: Annual

PREPARED FOR: U.S. Army Medical Research and Materiel Command
Fort Detrick, Maryland 21702-5012

REPORT DOCUMENTATION PAGE

Form Approved
OMB No. 0704-0188

1. AGENCY USE ONLY *(Leave blank)*	2. REPORT DATE	3. REPORT TYPE AND DATES COVERED
	August 1999	Annual (15 Jul 98 - 14 Jul 99)

4. TITLE AND SUBTITLE Immunobiological Aspects of erbB Receptors in Breast Cancer

5. FUNDING NUMBERS
DAMD17-96-1-6029

6. AUTHOR(S)
Mark I. Greene, M.D., Ph.D.

7. PERFORMING ORGANIZATION NAME(S) AND ADDRESS(ES)
University of Pennsylvania
Philadelphia, Pennsylvania 19104-3246

8. PERFORMING ORGANIZATION REPORT NUMBER

9. SPONSORING/MONITORING AGENCY NAME(S) AND ADDRESS(ES)
U.S. Army Medical Research and Materiel Command
Fort Detrick, Frederick, Maryland 21702-5012

10. SPONSORING/MONITORING AGENCY REPORT NUMBER

11. SUPPLEMENTARY NOTES

12a. DISTRIBUTION / AVAILABILITY STATEMENT
Approved for public release; distribution unlimited

12b. DISTRIBUTION CODE

13. ABSTRACT *(Maximum 200*

The general problem of assembly, activation and disabling the receptor complexes of the erbB family is being studied and its relevance to cancer ascertained. We have analyzed how mutants of the endodomain of p185neu affect the function of other heteromeric or homomeric partners of the receptor ensemble. We have studied molecular forms of neuregulin found in a transformed human lymphoid cell line that seem able to activate p185 even in the absence of erbB3 or 4.

We analyzed the creation of enabled or disabled receptor complexes built of the EGFR and mutant or normal forms of p185 to determine receptor inhibition pathways. Lack of an endodomain of p185 was found to disable the EGF receptor's kinase activity and limit transforming abilities even when additional ligands such as EGF were added. The biochemical pathway most inhibited was the PI3 kinase pathway. The scope of the major findings was that a component of the receptor complex called a signal inhibitory receptor polypeptide (SIRP) could be activated by the disabled complex and was, in part, responsible for limiting PI3 kinase activity. Finally, we are developing an understanding of receptor inhibition that involves complex activation of pathways such as SIRP and the modulation of proteasome function, in addition to receptor internalization.

14. SUBJECT TERMS	15. NUMBER OF PAGES
Breast Cancer erbB receptors	37
	16. PRICE CODE

17. SECURITY CLASSIFICATION OF REPORT	18. SECURITY CLASSIFICATION OF THIS PAGE	19. SECURITY CLASSIFICATION OF ABSTRACT	20. LIMITATION OF ABSTRACT
Unclassified	Unclassified	Unclassified	Unlimited

FOREWORD

Opinions, interpretations, conclusions and recommendations are those of the author and are not necessarily endorsed by the U.S. Army.

____ Where copyrighted material is quoted, permission has been obtained to use such material.

____ Where material from documents designated for limited distribution is quoted, permission has been obtained to use the material.

N/A Citations of commercial organizations and trade names in this report do not constitute an official Department of Army endorsement or approval of the products or services of these organizations.

N/A In conducting research using animals, the investigator(s) adhered to the "Guide for the Care and Use of Laboratory Animals," prepared by the Committee on Care and use of Laboratory Animals of the Institute of Laboratory Resources, national Research Council (NIH Publication No. 86-23, Revised 1985).

✓ For the protection of human subjects, the investigator(s) adhered to policies of applicable Federal Law 45 CFR 46.

N/A In conducting research utilizing recombinant DNA technology, the investigator(s) adhered to current guidelines promulgated by the National Institutes of Health.

N/A In the conduct of research utilizing recombinant DNA, the investigator(s) adhered to the NIH Guidelines for Research Involving Recombinant DNA Molecules.

____ In the conduct of research involving hazardous organisms, the investigator(s) adhered to the CDC-NIH Guide for Biosafety in Microbiological and Biomedical Laboratories.

Mark Ihre 8/9/99

PI - Signature Date

TABLE OF CONTENTS

(5) INTRODUCTION:

The objectives of these studies involved two major aims. The first aim was to gain a better understanding of the formation of homomeric or heteromeric ensembles of the $p185^{neu}$ or $p185^{c\text{-}neu}$ polypeptides and EGF receptors. The focus of this part of the effort was on the role of the endodomains of these molecules. The second aim was to clone the authentic ligand of the p185 molecules. We have made significant progress in both areas. The task order has been altered for aim 1 and is not yet at the predicted level for aim 2.

(6) BODY:

The first objective involved studying the mechanisms associated with $p185^{neu}$ or $p185^{c\text{-}neu}$ endodomains and the related signaling that was relevant to transformation or phenotype reversal. Deletion of the endodomain results in a trans-inhibitor of $p185^{neu}$ or $p185^{c\text{-}neu}$ polypeptides. These endodomain deletion mutants which we have termed trans-inhibitors also associate with all members of the erbB family and limit the formation of active kinase complexes. (3-7)

Attenuating mechanisms of signaling through erbB receptor tyrosine kinases (RTKs) in transformed cells have not been completely defined. Recent data indicate that Signal Regulatory Proteins (SIRPs, or murine SHPS-1), a family of membrane glycoproteins and putative substrates of the adaptor/effector SHP-2, modulate the activation of many RTKs, including the insulin receptor, the platelet-derived growth factor receptor, and the Epidermal Growth Factor Receptor (EGFR). SIRP/SHPS-1 proteins are tyrosine phosphorylated in response to EGF and insulin and were originally identified in anti-SHP-2 immunoprecipitates. (2)

SIRPα proteins are distinguished from SIRPβ forms by the presence of an endodomain containing immunoreceptor tyrosine-based inhibitory motifs (ITIMs), tyrosine phosphorylation sites which bind the SHP-2 phosphatase through SH2 interactions. (1,2)

We therefore sought to examine whether disabling an activated erbB receptor complex by a *trans*-inhibitory receptor mutant involves activation of SIRP proteins. We then addressed whether SIRP/SHPS-1 activation modulates cell growth, transformation and apoptosis observed in transformed neural cells in which erbB signaling is disabled.

Methods:

Vector Construction. Derivations of the carboxyl terminal-deleted T691stop p185neu mutant receptor construct have been detailed previously (1). The human SIRPα1 cDNA obtained in pRK5(RS) (1) was modified for eukaryotic expression. The pRK5(RS) plasmid was digested with NruI and XhoI, and the fragment containing the SIRPα1 gene was blunt-end ligated into the eukaryotic expression plasmid pIRESHyg (Clontech) previously linearized with BamHI and blunt-ended for ligation.

Maintenance of cells and transfection procedures. Human U87MG and A431 cells were obtained from the American Type Tissue Collection (Rockville, MD). Cell lines,

methods for deriving subclones expressing p185neu-derived proteins (T691stop neu-expressing derivatives), and transfection procedures have been detailed. (2-7) Characteristics of stable transfectants expressing T691stop neu mutant receptors have been detailed. (1) U87MG-derived cells expressing elevated amounts of EGFR (U87MG.wtEGFR cells) were obtained from Drs. H-J. Su Huang and Webster Cavenee, Ludwig Institute for Cancer Research, San Diego, CA. B104-1-1 cells expressing high levels of oncogenic p185neu were derived from NIH-3T3 fibroblasts, and M1 fibroblasts containing protooncogenic p185neu and human EGFR have been described.

For the analysis of SIRPα1 ectopic expression, cells were transfected either with empty vector (pIRESHyg) or pIRESHyg/SIRPα1 plasmids using lipofectamine followed by stable selection in hygromicin (80μg/ml). Positive SIRPα1 expressing subclones (U87/SIRPα1) were identified by western blotting using a polyclonal antibody reactive with SIRPα1. U87MG-derived clones expressing vector without insert were designated U87/pIRES cells.

Immunoprecipitation, co-immunoprecipitation and western blotting. Cells were seeded and allowed to attach overnight. After incubation with 5μg/ml anti-erbB receptor antibody (mAb 7.16.4 to B104-1-1 or M1 cells, and mAb 528 to U87MG or U87MG.wtEGFR cells) for 2h at 37°C, the medium was quickly aspirated and cells were washed twice with ice-cold PBS. Whole cell extracts were prepared by solubilization in PI/RIPA buffer for 30min at 4°C. After normalization of lysates derived from untreated cells and treated cells by Bio-Rad protein concentration assay, 500-1000μg of each cell lysate was incubated with 3μg of a carboxyl-terminal SHP-2 (SHPTP2) polyclonal antibody (Santa Cruz Biotechnology) or polyclonal antibody 116 reactive with the cytoplasmic domain of SHPS-1 (gift from Dr. A. Veillette). Immunocomplexes were then pulled down by addition of Protein-A conjugated to Sepharose 4B (Sigma). Independent samples treated with anti-receptor mAb to which protein A-Sepharose 4B alone was added (without SHP-2 antibody) were also included in some experiments as another control. The resulting immunoprecipitates were then subjected to SDS-polyacrylamide gel electrophoresis (PAGE), and then transferred onto nitrocellulose membranes. Protein phosphorylation was determined by western blot analysis with an anti-phosphotyrosine mAb, PY-20 (Santa Cruz Biotechnology), and visualized using the ECL detection system (Amersham). To identify co-immunoprecipitated SIRP/SHPS-1 proteins, membranes were reprobed either with a polyclonal anti-SIRP antibody generated against a SIRPα carboxyl-terminal fusion protein or the anti-SHPS-1 polyclonal antibody 114 (reactive with the first Ig-like domain of mouse SHPS-1, gift from Dr. A. Veillette).

For western blots evaluating Bcl-X_L protein levels, cells were harvested at indicated time points after irradiation, and samples were boiled in lysis buffer, as recommended by the Bcl-X_L antibody producer's manual. After normalization by the Bio-Rad (Hercules, CA.) protein concentration assay, proteins were separated by 12% SDS-PAGE.

In vitro kinase Assays. Details have been described previously (7) with modifications of the in vitro kinase assay for MAPK activity as performed by others. (1)

PI3 kinase Assay. Cells were seeded and left to attach overnight. One million cells were incubated with or without 50ng/ml of EGF for 5 min at 37°C, medium was

quickly aspirated, and cells were washed 2 times with ice-cold PBS. Whole cell extracts were prepared by solubilization in lysis buffer for 30 min at 4°C. After normalization for protein concentration, equal amounts of protein from cell extracts were immunoprecipitated with anti-phosphotyrosine 4G10 or anti-SHP2. Immunocomplex attached beads were washed twice with lysis buffer, twice with wash buffer, twice with reaction buffer, and resuspended in 40ul of reaction buffer containing a substrate mixture of phosphatidylinositol and phosphatidylserine and dispersed by sonication. The tubes were incubated at room temperature for 10 min and reactions were initiated by adding 5 uCi of [γ-^{32}P] ATP per reaction in 10 ul of 500uM ATP and terminated by addition of 80 ul of chloroform:methanol (1:1) after another 10 min. Phospholipids were extracted, dessicated and redissolved. The samples were chromatographed on thin layer chromatography (TLC) plates. Spots corresponding to phosphatidylinositol 3-phosphate were visualized by autoradiography.

Cell growth and Transformation assays. For cell growth, we utilized the MTT (3,(4,5-dimethylthiazol-2-yl)2,5-diphenyl-tetrazolium bromide) assay. (1) For assays of focus formation of stably transfected subclones, previous methods were employed.

Nuclei Staining and morphologic analysis of apoptosis. Irradiation and morphologic detection of apoptotic nuclei was performed as described. (4) Statistical significance of the data was determined using the Student's *t*-test.

Antibodies. The monoclonal antibody (mAb) 7.16.4 reactive against the p185neu ectodomain has been described previously. (1,4) mAb 528 reactive with the human EGFR was obtained from Oncogene Science (Uniondale, N.Y.). Anti-ERK and anti-JNK antibodies were obtained from Santa Cruz Biotechnology (Santa Cruz, CA). A polyclonal antibody reactive with the SHP-2 carboxyl terminus previously used to precipitate SHP-2/SIRP complexes was obtained from Santa Cruz Biotechnology. The anti-SHP2 antibody used for immunoblotting was obtained from Transduction Laboratories (Lexington, Ky.). Anti-phosphotyrosine mAb PY-20 was obtained from Santa Cruz Biotechnology.

Antibodies reactive with murine SHPS-1 (numbers 114 and 116) were kindly provided by Dr. Andre Veillette (McGill University, Montreal, Quebec, Canada).

GST-jun (Santa Cruz Biotechnology, Santa Cruz, CA) and myelin basic protein (MBP, Upstate Biotechnology) served as substrates for *in vitro* kinase reactions.

The bcl-X_L polyclonal antibody was obtained from Transduction Laboratories.

Results and Discussion:

In SHP-2 immunocomplexes, *trans*-inhibition of EGFR signaling by an endodomain deficient truncated p185neu receptor (T691stop) resulted in increased basal and EGF-induced tyrosine phosphorylation of SIRPα proteins of Mr=110kDa (not shown). An antibody reactive with the SIRPα carboxyl terminus showed that two endogenous SIRPα proteins of 95-110kDa co-precipitated with SHP-2 in EGFR-positive U87MG human glioma cells. The slower migrating form of SIRPα (110kDa) was differentially phosphorylated. SIRPα proteins contained in basal and EGF-stimulated SHP-2 complexes were comparable. Anti-SIRPα immunoprecipitates also showed that

T691stop expression increased SIRP pTyr content. In A431 cells previously used to identify SIRP family proteins (2), SIRPs complexed to SHP-2 migrated at the same mobility as in U87MG cells. Direct western blotting of A431 whole cell lysates with an anti-SIRPα antibody reactive with the carboxyl terminus also identified endogenous SIRPα proteins of 95-110 kDa (data not shown).

In order to investigate whether SIRP function may contribute to reduced cell growth, transformation and increased apoptosis previously observed in EGFR-disabled transformed neural cells we overexpressed the SIRPα1 cDNA in U87MG human glioma cells. (See Fig. 1) Unexpectedly, *in vitro* kinase assays showed that EGF-induced activation of extracellular signal-regulated kinase (ERK)-1, ERK-2, c-jun amino-terminal kinase (JNK) were comparable in SIRPα1-overexpressing transformed human cells when compared to cells expressing vector without insert. Notably, basal ERK activities between U87MG parental, U87/ SIRPα1 and U87/T691 derivatives were comparable. Interestingly, cell growth after 48h as determined by the MTT assay (Fig. 1A) was unaffected by overexpression of SIRPα1 in U87MG cells. Differences in cell growth were also not observed in SIRPα1-overexpressing cells in full growth media for up to seven days (data not shown).

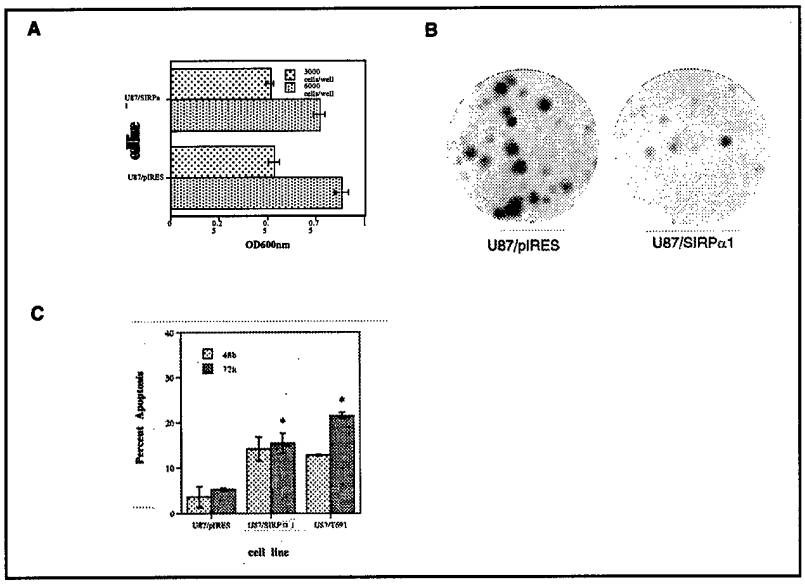

Fig. 1 A. Cell growth at 48 hr in 10% FBS-DMEM was evaluated using the MTT assay with U87/pIRES and U87/SIRPα1 cells. Results (mean±SD) of absorbance as determined by an ELISA reader are displayed for 2 cell concentrations and were in the linear range for this cell type. No differences in cell growth between U87/pIRES and U87/SIRPα1 cells were observed in this MTT assay. B. Transforming efficiency of SIRPα1-overexpressing U87MG-deived subclones. 200 U87MG-derived cells were plated with 10^4 NR6 cells and grown in 5% FBS-DMEM for 18-21 days. Foci (mean±SD) were then stained and quantitated based on triplicate dishes for each cell line. C. Induction of apoptosis following gamma-irradiation in U87MG human glioblastoma derivatives. Mean±SD of counts derived from 2 independent observers are presented as a percentage. Over 600 cells were counted in multiple fields for each sample after staining with 4',6-diamidino-2-phenylindole dihydrochloride hydrate (DAPI). At 72 hr following irradiation, levels of apoptosis were significantly (*) higher in U87/SIRPα1 cells ($p<.05$) and in U87/T691 cells ($p<.005$) than in control U87/pIRES cells.

Stable clones expressing elevated amounts of the SIRPα1 protein were inhibited 65% in the formation of morphologically transformed foci (Fig. 1B), as compared to clones expressing vector without insert (mean number of foci ± SD: U87/pIRES 31±1.4; U87/ SIRPα1 11 ± 2.8; data confirmed in three independent experiments). Elevated SIRPα1 expression thus inhibited the transformed phenotype in transformed cells containing multiple somatic alterations in addition to inhibiting transformation induced by a single oncogene product. Our preliminary studies showed that SIRP function contributes to reduced transformation mediated by the T691stop mutant receptor, but the inhibition was not related to diminution of MAP kinase activities. (Not shown) Rather, as shown in Fig. 2, we noted that the lipid kinase PI3 kinase had diminished activity in SIRP transfected cells.

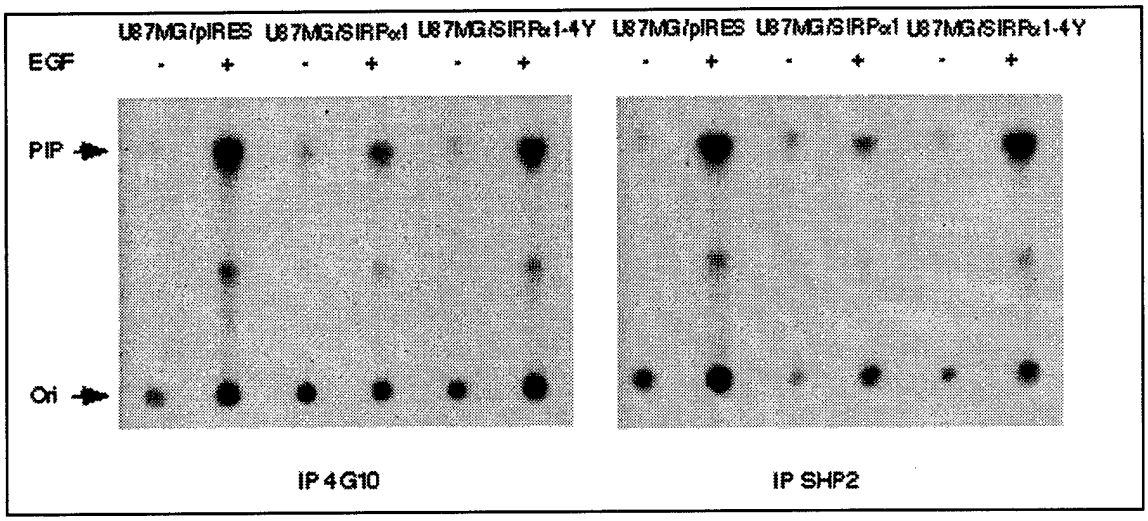

Fig. 2. EGF induced PI3 Kinase Activity. One million cells were treated with or without EGF (50ng/ml) for 5 min following a period of serum starvation of 24hr. Equal amounts of cell extracts were immunoprecipitated with Anti-PTyr 4G10 (A) or Anti-SHP2 (B). The resulting immunoprecipitates were analyzed for PI3 kinase activity as described in "Methods". An autoradiograph of a thin layer chromatograph is shown. The positions of origin (Ori) and phosphatidylinositol 3-phosphate (PIP) were indicated by arrows. SIRP1-4Y is a mutated form of SIRP (This mutant was provided by Axel Ullrich) that lacks carboxy terminus tyrosines and is not able to mediate inhibition of transformation. The gels clearly show that SIRP mediates its effect by inhibiting the lipid kinase PI3 kinase. Forms of SIRP which lack certain tyrosines (SIRP1-44) are unable to mediate this effect.

Prolonged serum deprivation (96h) did not induce apoptosis in transformed U87MG parental cells or U87/ SIRPα1 subclones, supporting previous observations in transformed neural cells. However, overexpression of the SIRPα1 cDNA conferred increased sensitivity to apoptosis following gamma-irradiation as determined by an examination of nuclear morphology following staining with 4',6-Diamidino-2-phenylindole dihydrochloride hydrate (DAPI) (Figs. 1C, 3). Apoptosis in U87/ SIRPα1 and U87/T691 cells was increased above U87/pIRES cells expressing vector without insert at both 48hr and 72hr following irradiation in full growth medium (mean percent apoptosis ± SD: U87/pIRES 3.6± 2.3, 48hr, 5.3± 0.4, 72hr; U87/ SIRPα1 14.2 ± 2.6, 48hr,

15.5 ± 2.1, 72hr; U87/T691 12.9 ± 0.2, 48hr, 21.5 ± 0.7, 72hr; these results were confirmed in three independent experiments) (Fig. 1C). Interestingly, apoptosis of irradiated U87/SIRPα1 cells was not enhanced by serum deprivation (data not shown), suggesting the activation of a pathway that is serum-independent.

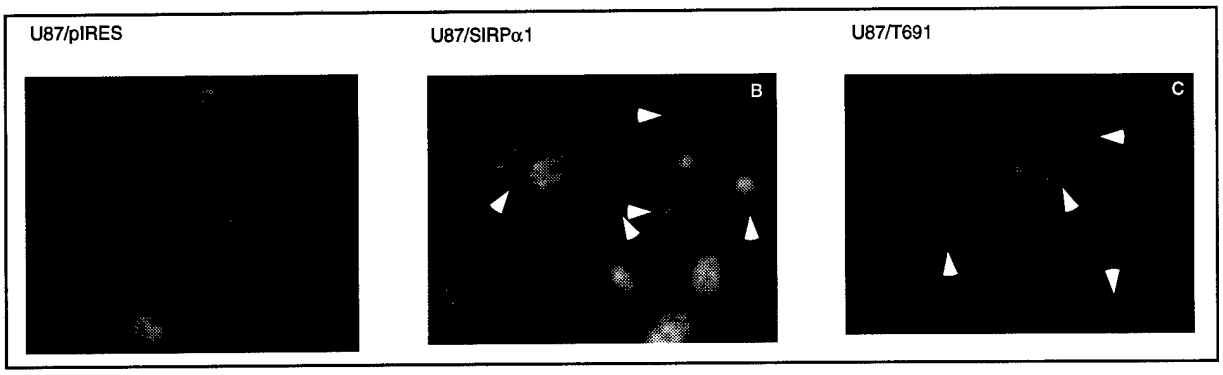

Fig. 3. Morphologic assessment of apoptosis in human glioma subclones following gamma-irradiation (10Gy). All cells were stained with DAPI 48-72 hr after being exposed to gamma-irradiation. U87MG cells overexpressing empty vector (A), SIRPα1 (B), and T691stop neu mutant receptors (C) are shown. Nuclei exhibiting apoptotic morphology are indicated by arrows.

Apoptosis occurring in SIRPα1-overexpressing cells may result from reduced levels of the bcl-X_L protein. Bcl-X_L was induced following gamma-irradiation in U87MG-derived cells. Interestingly, basal and radiation-induced levels of bcl-X_L protein were reduced in U87/SIRPα1 cells relative to controls (not shown). Bcl-X_L levels returned to baseline 72hr following irradiation in U87/SIRPα1 cells, while cells expressing vector without insert showed sustained elevation in bcl-XL protein levels 24-72hr following gamma-irradiation. Modulation of Bcl-X_L protein levels has been shown to influence sensitivity to apoptosis in tumor cells treated with chemotherapeutic drugs and in keratinocytes exposed to cell death signals.

Trans-receptor inhibition by constitutive expression of mutant p185neu forms results in reduced pTyr content of endogenous EGFR and p185neu proteins. (3-7) Our data suggest that one physiological stimulus for the tyrosine phosphorylation and activation of SIRP proteins is the inhibition of erbB signaling by some as yet unidentified kinase. Increased SIRPα function results in reduced transformation and increased apoptosis following irradiation in erbB-inhibited transformed cells. We have previously demonstrated a correlation between reduced transformation and increased sensitivity to gamma-irradiation. Furthermore, our studies suggest that SIRP functions by disabling PI3 kinase more so than modulating raf-MAPKinase activity. These findings support our previous efforts. (7)

In our original efforts on objective 2, to clone the NAF (neu-specific activating factor) activity (11,12) from the ATL-2 cell line (14,16), we surmised that NAF may be a novel member or isoform of the neuregulin gene family. We identified several conserved regions between the neuregulin-1 (NRG-1) and neuregulin-2 (NRG-2) genes and

designed primers that correspond to these conserved sequences. The NRG-1 and NRG-2 gene products originate as membrane spanning precursors whose extracellular domains are proteolytically cleaved to liberate soluble forms of the neuregulins. (13,17) The IgG-like domain, EGF-like domain, and transmembrane spanning domain were the most conserved between the NRG-1 and NRG-2 pre-pro forms, so primers corresponding to these domains were generated for our RT-PCR analysis.

In the last update we reported that we were successful using the primers corresponding to the NRG transmembrane domain and were able to identify that a NRG-2-related gene (8,9,10) could be detected in the ATL-2 cDNA population. We used this probe to screen an oligo-dt primed ATL-2 cDNA library. However, in this round of cDNA library screening we only identified several false positives using the transmembrane domain as a probe. We feel the short length of this probe (only 100 nucleotides in length) and the possible promiscuity of the probe binding to any clone that has transmembrane spanning regions has caused us to obtain inappropriate clones in our first round of ATL-2 cDNA library screening.

Therefore, we needed to become more aggressive with our RT-PCR efforts so that we could obtain a larger fragment of the NRG-2$_{ATL-2}$ molecule that we are pursuing. New primers were designed that correspond exactly to conserved regions outside the region encoding the transmembrane domain. Using this renewed RT-PCR strategy, we were able to amplify a clone, designated 'SK1', approximately 1000 nucleotides in length that extends from the middle of the immunoglobulin-like domain to just beyond the transmembrane region and into the intracellular domain of the NRG-2$_{ATL-2}$ molecule from the ATL-2 cDNA. The SK1 clone exactly matched the reported sequence for the corresponding region of the NRG-2 sequence (9,10,13) in the Genbank database. This suggested that the NRG-2$_{ATL-2}$ molecule is an isoform of NRG-2 and apparently not a new neuregulin-related gene.

However, we still need to clone the entire NRG-2$_{ATL-2}$ gene to determine whether it encodes a distinct isoform that may correspond to the NAF activity. Most specifically, we have not yet identified the amino terminal sequences of the NRG-2$_{ATL-2}$ gene we are studying. It is the amino terminal sequences of neuregulin gene products that are the region that contains the most significant diversity with regard to the generation of physiologically distinct isoforms from a single neuregulin gene. The amino terminal domain along with the EGF-like domain confer the specificity of binding to erbB receptors and, in part, may dictate the differential heteromer-inducing potential induced by different neuregulin isoforms. For example, the amino terminal domain of the NRG-1 gene product can contain 26 distinct amino acids (for ARIA), or 219 distinct amino acids (for GGF-II), or 34 distinct amino acids (for heregulin/NDF) proximal to the IgG-like domain resulting in three biochemically and functionally distinct forms of the NRG-1 gene product.

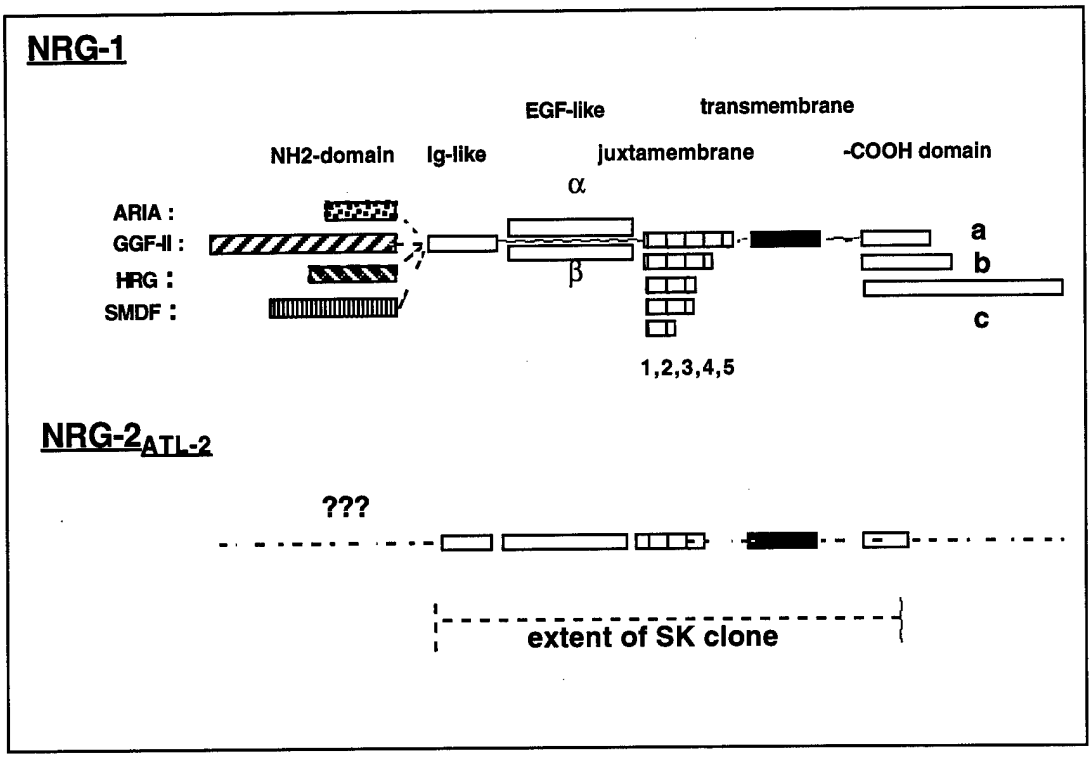

Schematic of partial NRG-2ATL-2 'SK' sequence and comparison with NRG-1 isoforms.

Currently, we are employing two methods to identify the amino-terminal coding sequence for the NRG-2ATL-2 molecule to determine whether we have identified a novel isoform of NRG-2 that may correspond to the NAF activity in the ATL-2 cells. 5'-RACE analysis and the use of the SK1 probe to screen ATL-2 cDNA libraries are both underway. NRG-2-specific primers are now being used to generate cDNA for RACE analysis and to generate new cDNA libraries that are enriched in NRG-related sequences from ATL-2 cells and from other tissues. We have other tissues that we feel may potentially contain neu protein-specific molecules. Random primed and NRG-2-specific primed cDNA libraries were generated for searching for the amino terminal region/full-length NRG-2ATL-2 molecule. These cDNA libraries have been generated and are being amplified. Preliminary screening of a small portion of the pre-amplified random primed ATL-2 cDNA library was performed and several candidate signals were observed in short autoradiographic exposures.

In the event that the NAF activity is not due to a novel neuregulin-related gene or isoform, we have started to use an expression cloning approach that has been developed using the IL-3 dependent 32-D myeloid cell line. (15) In the absence of IL-3, it was shown that certain growth factor signaling pathways can substitute for the IL-3-dependent mitogenicity in these cells. Namely, when the EGFR was transfected into the 32-D cell line, EGF treatment of the EGFR-bearing transfectants was able to sustain 32-D

cell growth and prevent apoptosis. (8) Therefore, we have obtained 32-D cells that have been transfected with the $p185^{c\text{-}erbB2}$ protein. Bulk transfection of these $p185^{c\text{-}erbB2}$-bearing cells with cDNAs from tissues thought to express candidate neu-specific activating activity (such as the ATL-2 cells or neural tissues) would, in some of the transfected cells, result in co-expression of $p185^{c\text{-}erbB2}$ and a candidate ligand. In the absence of the IL-3-dependent mitogenicity, the co-expression of a candidate ligand with the $p185^{c\text{-}erbB2}$ protein would, through autocrine activation of the $p185^{c\text{-}erbB2}$-mediated mitogenic potential, allow the clonal expansion of these cells and prevent their apoptosis. In this manner, this assay may facilitate both the specific search for an $p185^{c\text{-}erbB2}$-specific ligand in ATL-2 cells or in other tissue contexts.

We have accelerated our sixth task and have focused on defining a pathway activated by endodomain deletion mutants of p185. In the set of studies performed, we showed that endodomain deletion mutants led to post-translational modification of a molecule called Signal Inhibitory Receptor Polypeptide (SIRP), and this affects PI3 kinase function.

The level of accomplishment of tasks 4 and 5 is less than expected. The cloning of the 5′ end of the NAF-neuregulin type of cDNA species has been problematic. However, we have, nevertheless, made significant progress in this area and should complete all of the proposed tasks in the next year.

(7) KEY RESEARCH ACCOMPLISHMENTS:

- Defining the role of endodomain mutants of the p185 polypeptide
- Defining an inhibitory pathway that is dependent on SIRP
- Showing SIRPs affect the lipid kinase/PI3 kinase
- Progress in identifying new isoforms of ligands

(8) REPORTABLE OUTCOMES:

Publications

O'Rourke, D., Kao, G.D., Singh, N., Park, B., Muschel, R.J., Wu, C. and Greene, M.I.: Conversion of a radioresistant phenotype to a more sensitive one by disabling erbB receptor signaling in human cancer cells. Proc. of the Nat'l Acad. of Sci. (USA), 95:10842-10847, 1998.

Qian, X., O'Rourke, D.M., Fei, Z., Zhang, H., Kao, C. and Greene, M.I.: Domain-specific interactions between the $p185^{neu}$ and epidermal growth receptor kinases determine differential signaling outcomes. Journal of Biological Chemistry, 274(2):574-583, 1999.

Park, B., O'Rourke, D., Wang, Q., Davis, J., Post, A., Qian, X. and Greene, M.I.: Induction of the Tat-binding protein-1 accompanies the disabling of oncogenic erbB receptor tyrosine kinases. Proc. of the Nat'l Acad. of Sci. (USA), 96:6434-6438, 1999.

Chih-Ching Kao received Ph. D., Thesis title: Studies of the interaction of novel forms of the $p185^{c\text{-}neu}$ receptor ectodomain.

(9) CONCLUSIONS:

One of our original hypotheses was that mutating or deleting p185 endodomains might develop biochemical insight into the formation of inactive receptor complexes and help define signaling events that were initiated to reverse phenotype. We have now shown that transinhibition by an endodomain mutant affects SIRP (Signal Inhibitory Receptor Polypeptides) signaling in these preliminary studies. Differential associations between endogenous proteins involving SIRP and PI3 kinase influence transformation and apoptosis in erbB-expressing cells. One implication of the observation that transmembrane SIRP proteins are activated in response to inhibition of erbB receptor signaling would be the design of therapies which directly activate a SIRP inhibitory pathway and thus reduce transformation and increase apoptosis following the induction of genomic damage.

All neuregulins found to date bind to erbB3 or erbB4 with moderate affinity. Some studies have suggested that there is an asymmetric low affinity binding of certain neuregulin species to erbB2/neu permitting binding of ligand simultaneously to erbB2/neu and its heteromeric partner.

We suspect that the ATL2 neuregulin form may have better binding to erbB2. If this species, when expressed, fulfills this criteria, it would change our thinking of how neu mediates its activities in many situations such as breast cancer. Therefore, identifying if NAF truly activates $p185^{c\text{-}neu/erbB2}$ alone is an important step in understanding breast cancer pathogenesis.

(10) REFERENCES

1. Qian, X., O'Rourke, D. M., Zhao, H., and Greene, M. I. (1996) *Oncogene* **13**, 2149-2157.

2. Kharitonenkov, A., Chen, Z., Sures, I., Wang, H., Schilling, J., and Ullrich, A. (1997) *Nature* **386**, 181-186.

3. Fujioka, Y., Matozaki, T., Noguchi, T., Iwamatsu, A., Yamao, T., Takahashi, N., Tsuda, M., Takada, T., and Kasuga, M. (1996) *Mol Cell Biol* **16**, 6887-6899.

4. O'Rourke, D. M., Qian, X., Zhang, H.-T., Davis, J. G., Nute, E., Meinkoth, J., and Greene, M. I. (1997) *Proc. Natl. Acad. Sci. (USA)* **94**, 3250-3255.1998.

5. O'Rourke, D. M., Nute, E. J. L., Davis, J. G., Wu, C., Lee, A., Murali, R., Zhang, H.-T., Qian, X., Kao, C.-C., and Greene, M. I. (1998) *Oncogene* **16**, 1197-1207.

6. Qian, X., Dougall, W. C., Hellman, M. E., and Greene, M. I. (1994) *Oncogene* **9**, 1507-1514.

7. Qian, X., O'Rourke, D. M., Fei, Z., Kao, C.-C., Zhang, H.-T., and Greene, M. I. (1999) *J Biol Chem* **274**, 574-583.

8. Alimandi, M., Wang, L.-M., Bottaro, D., Lee, C.-C., Kuo, A., Frankel, M., Fedi, P., Tang, C., Lippman, M. and Pierce, J.H. (1997) *EMBO* **16**, 5608-5617.

9. Carraway, K., Weber, J.L., Unger, M.J., Ledesma, J., Yu, N., Gassmann, M. and Lai, C. (1997) *Nature*. **387**, 512-516.

10. Chang, H., Riese, D., Gilbert, W., Stern, D. and McMahan, U. (1997) *Nature* **387**, 509-512.

11. Davis, J.G., Hamuro, J., Shim, C.Y., Samanta, A., Greene, M.I. and Dobashi, K. (1991) *Bioch. Biophys. Res. Comm.* **179**, 1536-1542.

12. Dobashi, K., Davis, J.G., Mikami, Y., Freeman, J.K., Hamuro, J. and Greene, M.I. (1991) *Proc. Nat'l. Acad. Sci.* **88**, 8582-8586.

13. Higashiyama, S., Horikara, M., Yamada, K., Ichino, N., Nakano, N., Nakagawa, T., Miyagawa, J., Matsushita, N., Nagatsu, T., Taniguchi, N. and Ishiguro, H. (1997) *Moll. Cell. Biol.* **122**, 675-680.

14. Maeda, M., Shimuzu, A., Ikuta, K., Okamata, H., Kashiwara, M., Uchiyama, T., Honjo, T. and Yodoi, J. (1985) *J. Exp. Med.* **162**, 2169-2174.

15. Pierce, J.H., Ruggerio, M., Fleming, T.P., DiFiore, P. P., Greenberger, J.S., Varticovski., L., Schlessinger, J., Rovera, G. and Aaronson, S.A. (1988) *Science* **239**, 628-631.

16. Teshigawara, K., Maeda, M., Nishino, K., Nikaido, T., Uchiyama, T., Tsudo, M., Wano, Y. and Yodoi, J. (1985) *J. Moll. & Cell. Immunology.* **2**, 17-26.

17. Zhang, D., Frantz, G. and Godowski, P.J. (1998) *Molecular Pyschiatry* **3**, 112-115.

Conversion of a radioresistant phenotype to a more sensitive one by disabling erbB receptor signaling in human cancer cells

(apoptosis/epidermal growth factor receptor/glioblastoma/p185neu/*trans*-receptor inhibition)

DONALD M. O'ROURKE*†‡§, GARY D. KAO¶, NATASHA SINGH†, BYEONG-WOO PARK†, RUTH J. MUSCHEL†¶, CHUAN-JIN WU†, AND MARK I. GREENE†‡

Departments of *Neurosurgery, †Pathology and Laboratory Medicine, ¶Radiation Oncology and ‡Cancer Center, University of Pennsylvania School of Medicine, Philadelphia, PA 19104

Proc. Natl. Acad. Sci. USA
Vol. 95, pp. 10842–10847, September 1998
Medical Sciences

Proc. Natl. Acad. Sci. USA
Vol. 95, pp. 10842–10847, September 1998
Medical Sciences

Conversion of a radioresistant phenotype to a more sensitive one by disabling erbB receptor signaling in human cancer cells

(apoptosis/epidermal growth factor receptor/glioblastoma/p185neu/*trans*-receptor inhibition)

DONALD M. O'ROURKE*†‡§, GARY D. KAO¶, NATASHA SINGH†, BYEONG-WOO PARK†, RUTH J. MUSCHEL†¶, CHUAN-JIN WU†, AND MARK I. GREENE†‡

Departments of *Neurosurgery, †Pathology and Laboratory Medicine, ¶Radiation Oncology and ‡Cancer Center, University of Pennsylvania School of Medicine, Philadelphia, PA 19104

Communicated by James M. Sprague, University of Pennsylvania School of Medicine, Philadelphia, PA, June 12, 1998 (received for review March 6, 1998)

ABSTRACT **Inhibition of cell growth and transformation can be achieved in transformed glial cells by disabling erbB receptor signaling. However, recent evidence indicates that the induction of apoptosis may underlie successful therapy of human cancers. In these studies, we examined whether disabling oncoproteins of the erbB receptor family would sensitize transformed human glial cells to the induction of genomic damage by γ-irradiation. Radioresistant human glioblastoma cells in which erbB receptor signaling was inhibited exhibited increased growth arrest and apoptosis in response to DNA damage. Apoptosis was observed after radiation in human glioma cells containing either a wild-type or mutated p53 gene product and suggested that both p53-dependent and -independent mechanisms may be responsible for the more radiosensitive phenotype. Because cells exhibiting increased radiation-induced apoptosis were also capable of growth arrest in serum-deprived conditions and in response to DNA damage, apoptotic cell death was not induced simply as a result of impaired growth arrest pathways. Notably, inhibition of erbB signaling was a more potent stimulus for the induction of apoptosis than prolonged serum deprivation. Proximal receptor interactions between erbB receptor members thus influence cell cycle checkpoint pathways activated in response to DNA damage. Disabling erbB receptors may improve the response to γ-irradiation and other cytotoxic therapies, and this approach suggests that present anticancer strategies could be optimized.**

The molecular parameters that determine how a cell becomes more or less sensitive to DNA damage induced by radiation or chemotherapeutic agents are poorly understood. Status of cell cycle checkpoint-signaling pathways has been argued to be an important determinant of the response to DNA damage, and mutations in checkpoint components are prevalent in human cancers (reviewed in refs. 1 and 2). A recently introduced paradigm suggests that tumor cells exhibit growth arrest or apoptosis in response to cytotoxic therapies depending on the functional state of checkpoint pathways and that radiation-induced apoptosis may result from impaired growth arrest pathways (3). Similarly, in other systems using nontransformed cells, incomplete mechanisms of DNA repair, occurring during checkpoint phase delay, increase the tendency to apoptosis (4).

Human glioblastomas exhibit many genetic alterations, including amplification and/or mutation of the gene encoding the epidermal growth factor receptor (EGFR) (reviewed in refs. 5 and 6) in some cases resulting in expression of a constitutively activated EGF receptor kinase (7–9). We have shown that expression of a *trans*-receptor inhibitor of the EGFR, derived from the ectodomain of the p185neu oncogene (T691stop neu), forms heterodimers with both full-length EGFR and a constitutively activated extracellular-deleted mutant EGFR form (ΔEGFR) commonly observed in human glial tumors, particularly those of higher pathologic grade (9, 10). Cell growth and transformation of EGFR-positive or EGFR/ΔEGFR-coexpressing human glioma cells is inhibited by kinase-deficient deletion mutants of p185neu (9, 10). The surface-localized T691stop neu mutant/EGFR heterodimeric receptor complex has decreased affinity for the EGF ligand, impaired internalization kinetics, reduced phosphotyrosine content, and diminished enzymatic kinase activity relative to full-length EGFR and ΔEGFR homodimeric complexes (9, 10).

The specific pathways mediating oncogenic transformation in EGFR positive-transformed human cells have not been characterized completely. Naturally occurring ΔEGFR oncoproteins may increase constitutive activity of a Grb2/Shc/Ras pathway (11) and signaling through phosphatidyl inositol-3 (PI-3) kinases (12), presumably by binding to distinct adaptor proteins (13). Particular mitogen-activated protein kinases, such as those of the c-jun amino terminal kinase family, may be constitutively activated by ligand-independent oncogenic ΔEGF receptors (14). Although holo-EGFRs have been found to be weakly transforming only in a ligand-dependent manner at high levels of receptor expression in fibroblasts, many human tumors exhibit elevated levels of EGFR and this may contribute to unregulated kinase activity in transformed cells (15, 16).

We sought to address whether specific inhibition of signaling through the overexpressed EGFR in radioresistant human glioma cells would alter the physiologic response of these cells to the induction of genomic damage. γ-irradiation combined with erbB receptor inhibition resulted in a greater degree of radiation-induced growth arrest and apoptosis in cancer cells normally resistant to ionizing radiation. These results have implication for the design of receptor-specific agents capable of sensitizing cells to cytotoxic therapies and suggest that erbB receptor-specific inhibition combined with cytotoxic treatments may improve the response to anticancer regimens.

MATERIALS AND METHODS

Vector Construction. The derivation of the T691stop neu mutant receptor construct has been detailed previously (10).

The publication costs of this article were defrayed in part by page charge payment. This article must therefore be hereby marked "*advertisement*" in accordance with 18 U.S.C. §1734 solely to indicate this fact.

Abbreviations: DAPI, 4′,6-diamidino-2-phenylindole dihydrochloride hydrate; EGFR, epidermal growth factor receptor; RT, radiation treatment.

§To whom reprint requests should be addressed. e-mail: orourked@mail.med.upenn.edu.

Maintenance of Cells and Development of Stably Transfected Cell Lines. The U87MG human glioblastoma cell line was obtained from Webster Cavenee (Ludwig Cancer Institute, San Diego). U373MG human glioma cells, originally isolated from a human anaplastic astrocytoma, were obtained through the American Type Tissue Collection (ATCC; Rockville, MD). Maintenance of cells lines, methods for deriving subclones expressing p185neu-derived proteins and transfection procedures have been described previously (9, 10).

Flow Cytometric Analysis of Cell Cycle Distribution. Cells were stained for flow cytometry by sequential treatment with 0.003% trypsin solution, followed by 0.05% trypsin inhibitor, 0.01% RNase A solution, and then 0.0416% propidium iodide and 5 mM spermine tetrachloride solution. Each treatment was performed for 10 min with continuous shaking at room temperature. All reagents were ordered from Sigma. Cell cycle analysis was performed within 2 h of staining on a Becton Dickinson FACScan flow cytometer. Ten thousand events were collected for each sample and the data analyzed by using the MODFIT cell cycle analysis program (Becton Dickinson, version 2.0).

Nuclei Staining and Morphologic Analysis of Apoptosis. Cells were plated onto coverslips for at least 12 h before irradiation. Irradiation was performed in conditions identical to the colony formation assays. Coverslips were then washed twice with PBS at the indicated times and fixed in 50:50 mix of ice-cold methanol/acetone for 1 min. Coverslips were subsequently stained with 4′,6-diamidino-2-phenylindole dihydrochloride hydrate (DAPI) (Sigma) at a concentration of 0.1–.25 μg/ml in PBS. Inter-observer consistency in apoptosis counts was confirmed with terminal deoxynucleotidyl transferase-mediated dUTP nick end labeling-staining and by three independent observers.

Cell counts were performed within 30 min of staining, and photographs were taken on a Zeiss Axioplan epifluorescence microscope. At least three independent fields of 100 cells were counted for each sample.

Colony Formation Assay. Cell survival after irradiation was assessed by the colony formation assay. The number of cells to be plated was calculated to form 20–200 colonies per dish at each radiation dose and plated into 10-cm culture dishes (Fisher Scientific). By using a J. L. Shepherd (San Fernando, CA) model 30 Mark I Cesium-137 irradiator, 12.8 Gy/min of irradiation was delivered to the cells on a rotating platform to ensure uniform dosing. Cells were incubated after irradiation at 37°C with 5% CO_2 for 7–10 days and then stained with crystal violet. Colonies containing >50 cells were counted under a dissecting microscope. The surviving fraction is the ratio of the number of colonies formed to the number of cells plated and was corrected for plating efficiency. At least three cell concentrations were used for each radiation dose.

Western Blotting. For each time point, 10^5 cells per 6-cm plate were harvested by lysis in 400 μl of sample buffer (10% glycerol/2% SDS/100 mM DTT/50 mM Tris, pH 6.8). Thirty microliters of each lysate was loaded per lane and separated by electrophoresis on a 15% SDS-polyacrylamide gel before overnight transfer to a nitrocellulose membrane (Bio-Rad). Membranes were probed with mouse anti-human p53 mAb (NeoMarkers, Fremont, CA), followed by goat anti-mouse Ig secondary antibody coupled to horseradish peroxidase (Amersham). To reduce background antibody binding, incubation with secondary antibody in 2.5% powdered milk in PBS was performed. Detection was performed by enhanced chemiluminescence (ECL, Amersham). Relative levels of p53 expression were determined by scanning the blots using a scanning densitometer (Molecular Dynamics).

Antibodies. The mAb 7.16.4 reactive against the p185neu ectodomain has been described (10). Polyclonal antibodies reactive with p53 and p21 were obtained from NeoMarkers. Antibodies reactive with bcl-2, bax, and bcl-x_L were obtained from Oncogene Science.

RESULTS

Cell Cycle Distribution of Cycling Human Glioblastoma Cells Treated with γ-Irradiation: Effects of Disabling erbB Signaling on Growth Arrest. For both U87MG and U87/T691 cells, prolonged serum starvation alone (72–100 h) led to increased accumulation of cells in G_0/G_1, with modest reductions in both the S and G_2/M populations. U87/T691 cells exhibited a higher G_0/G_1 fraction than parental U87MG cells either in the presence of serum (Fig. 1 *A* and *C*) or after prolonged serum deprivation (data not shown). The relative increase in growth arrest induced by expression of the T691stop neu mutant receptor in U87MG cells was thus not overcome by growth in full serum.

Induction of growth arrest by exposure of asynchronously cycling transformed human glial cell populations to γ-irradiation was greater than that induced by prolonged serum deprivation alone. In both U87MG and U87/T691 cells, irradiation of cells grown under full serum growth conditions caused robust increases in G_0/G_1 and G_2/M, and a decrease in the percentage of cells in S phase, as determined by flow cytometric staining for DNA content (Fig. 1 *B* and *D*). Reduction of the S phase fraction and accumulation of cells in G_2 is characteristic of cells sustaining DNA damage (4, 17). The data in Fig. 1 depict a representative experiment of cells analyzed 72 h after γ-irradiation. Earlier time points indicated similar trends, but analysis 72 h after irradiation was chosen to be consistent with subsequent experiments (see below). An analysis of three independent experiments revealed the following changes in cell cycle distribution [mean percent of cells ± SEM; ± radiation treatment (RT)]: (*i*) U87MG parental cells: G_0/G_1: 26 ± 2.8, +RT 51.5 ± 2.1; S: 66 ± 4.2, +RT 21 ± 2.8; G_2/M: 8 ± 1.4, +RT 28.5 ± 0.7; (*ii*) U87/T691 cells: G_0/G_1: 34.5 ± 4.9, +RT 71 ± 7.1; S: 57.5 ± 4.9, +RT 16 ± 4.2; G_2/M: 7.5 ± 0.7, +RT 12.5 ± 3.5. U87/T691 cells exhibited a higher G_0/G_1 fraction and reduced S and G_2/M

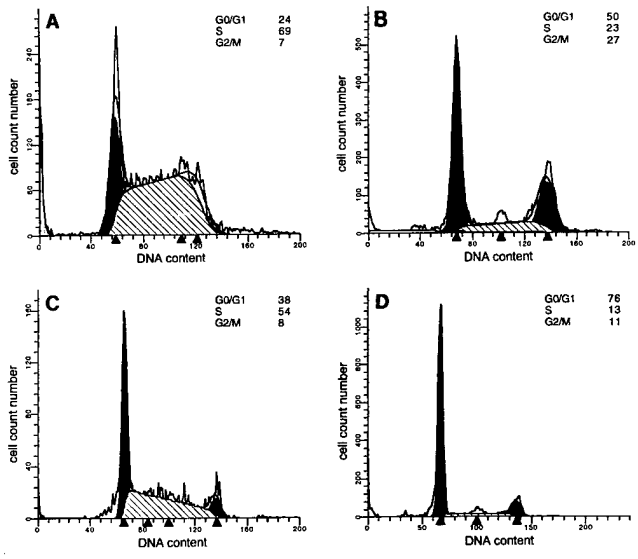

FIG. 1. Cell cycle distribution of human glioblastoma cells with or without radiation treatment in 10% serum. Parental U87MG cells (*A* and *B*) and U87/T691 transfectants (*C* and *D*) were studied. Cells were plated in 60-mm dishes and allowed to attach before either being γ-irradiated (10 Gy) (*B* and *D*) or mock-irradiated (*A* and *C*). After 72 h, cells were than analyzed by flow cytometry after propidium iodide staining. The distributions of cells according to DNA content are indicated in each panel. The data shown in this experiment are representative of four independent experiments.

populations when compared with parental glioblastoma cells when grown asynchronously in culture either with or without radiation treatment, and the largest difference was in the G_0/G_1 population. Radiation-induced increases in the G_2/M fraction were seen in both U87MG and U87/T691 cells, although to a greater degree in parental U87MG cells. Serum deprivation and radiation treatment in these cell populations was not additive and did not appreciably alter the cell cycle distributions in either cell line from that observed with radiation treatment in full serum (data not shown). Thus, disabling EGFR-mediated signaling appears to induce a growth arrest by a mechanism distinct from that observed with prolonged serum deprivation.

***Trans*-Receptor Inhibition Sensitizes Human Glioblastoma Cells to Radiation-Induced Apoptosis.** Human glioblastoma cells have been shown to be especially resistant to radiation treatment both experimentally and clinically. EGFR overexpression and/or mutation has been correlated with particularly aggressive human glial tumors and oncogenicity was suggested to be caused by reduced apoptosis *in vitro* and *in vivo* (18). We examined whether inhibition of EGFR-mediated signaling in human glioblastoma cells by the T691stop neu mutant receptor could sensitize cells to apoptotic cell death.

With prolonged serum deprivation, we observed only 0–1% apoptosis in U87MG parental cells by either 4′-6-diamidino-2-phenylindole (DAPI) staining or terminal deoxynucleotidyl transferase-mediated dUTP nick end-labeling staining, which was less than that observed in other studies (18). We found that U87MG-derived cells do not exhibit a sub-G_0 peak by flow cytometric analysis after propidium iodide staining under conditions causing apoptosis, which is in agreement with others (19). Expression of the T691stop neu inhibitor in U87MG cells resulted in only 0–2% apoptosis with prolonged serum deprivation as determined by immunohistochemical identification of apoptotic nuclei with DAPI.

Apoptosis was maximal in repeated studies at 72 h, and this time point was selected for all additional experiments. Expression of the T691stop neu protein in the U87MG cell background increased the level of radiation-induced apoptosis to 23 ± 7.9% (mean ± SEM) at 72 h in four independent experiments in full growth media (Fig. 2*A*). Prolonged serum deprivation combined with radiation resulted in 33 ± 10.6% apoptosis in U87/T691 cells and in 11 ± 1.5% apoptosis in parental U87MG cells, a comparable increase in both populations above that observed with radiation of cells in full growth media. These data indicate that T691stop neu expression induced greater apoptosis than prolonged serum deprivation in U87MG cells. The morphological changes of nuclear blebbing and fragmentation characteristic of apoptosis are shown by immunohistochemical analysis of U87MG-derived cultured cells stained with DAPI (Fig. 3*A–D*). The apoptotic indices represent an underrepresentation of total cell death after radiation in U87/T691 cells because we were unable to examine floating cells immunohistochemically.

Clonogenic Survival of Irradiated Human Glioblastoma Cells. We measured the number of cells that escape growth arrest or death and are able to go on to form a colony, an assay commonly used to determine radiosensitivity. In certain cases, clonogenic growth assays have not correlated with sensitivity to radiation or chemotherapy (3), presumably because the fate of the dead or stably arrested cells is not determined in this assay (20). As shown in Fig. 4, U87/T691 cells exhibited increased sensitivity to radiation across a range of radiation concentrations (2–10 Gy). U87/T691 cells were approximately one-half log more sensitive to radiation than their untransfected parental counterparts at all radiation doses tested. These data suggest a correlation between increases in growth arrest and apoptosis and increased radiosensitivity after inhibition of erbB signaling in irradiated human glioma cells. We

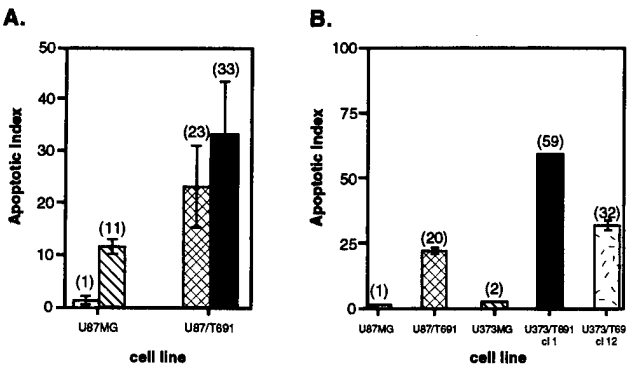

FIG. 2. Determination of apoptosis and clonogenic survival after γ-irradiation of human glioblastoma cells. (*A*) Cells were plated and allowed to attach before being exposed to γ-irradiation (10 Gy) in 10% serum or serum-free media. After 72 h, quantitation of apoptosis was conducted by two independent observers. The apoptotic index is the percentage of apoptotic cells with morphologic evidence of apoptosis as determined by staining of nuclei with DAPI. Results presented are mean ± SEM of four independent experiments, and the mean is indicated in parentheses. U87MG cells were grown in 10% serum (□) or serum-free media (▨) and U87/T691 cells were grown in 10% serum (▩) or serum-free media (■). (*B*) U87MG and U373MG human glioma cells and derivatives were stained with DAPI and analyzed for apoptotic morphology 72 h after γ-irradiation. The mean is indicated in parentheses, and the index shown in this representative experiment is mean ± SD. These results are representative of two additional experiments. Apoptotic indices were felt to be an underestimate because floating cells could not be assayed by this technique.

confirmed these results by analysis of additional T691stop neu-expressing subclones.

Relationship of Radiation Sensitivity of Human Glioblastoma Cells to p53 Status. U87MG cells and their derivatives contain wild-type p53 and p21 proteins. p53 status has been shown to influence the response to ionizing radiation in a number of transformed and nontransformed cell types (21–23). Western analysis of cell lysates obtained at distinct time points after radiation treatment indicated persistent increases in p53 protein levels detected at all times between 6 and 72 h after radiation in both U87MG and their T691stop neu-transfected derivatives (Fig. 5). The zero time point indicates cells which were γ-irradiated and immediately lysed for analysis. p53 densities were comparable at this time point to mock-irradiated, cycling cells (data not shown). We observed a 10-fold increase in p53 density 12 h after radiation in U87/T691 cells, as compared with only 1.5- to 3-fold increases in both U87MG cells and U87/T691 cells at all other time points examined. This trend was consistently observed (four experiments), and was seen in U87/T691 cells as early as 6 h after radiation in some experiments, and suggests that p53-dependent signaling pathways may be more efficiently activated by disabling the EGFR in the presence of genomic damage. Alterations in p53-regulated checkpoint proteins have been observed 12 h after the induction of genomic damage by γ-irradiation (24) Growth inhibition and differentiation of human breast cancer cells after ligation of erbB receptors has been associated with activation of a p53-dependent pathway (25).

p21 was induced in both U87MG and U87/T691 cells after radiation treatment, with highest levels seen 24 h after radiation exposure in both cell lines. In both U87MG cells and U87/T691 cells, p21 protein density 6–24 h after radiation was comparable (data not shown). Although others (18) have suggested that up-regulation of bcl-x_L is associated with reduced apoptosis in human glioma cells, we detected no changes in bcl-x_L protein expression after radiation in either U87MG or U87/T691 cells. Both constitutive and radiation-induced bcl-x_L levels were comparable in U87MG and U87/T691 cells

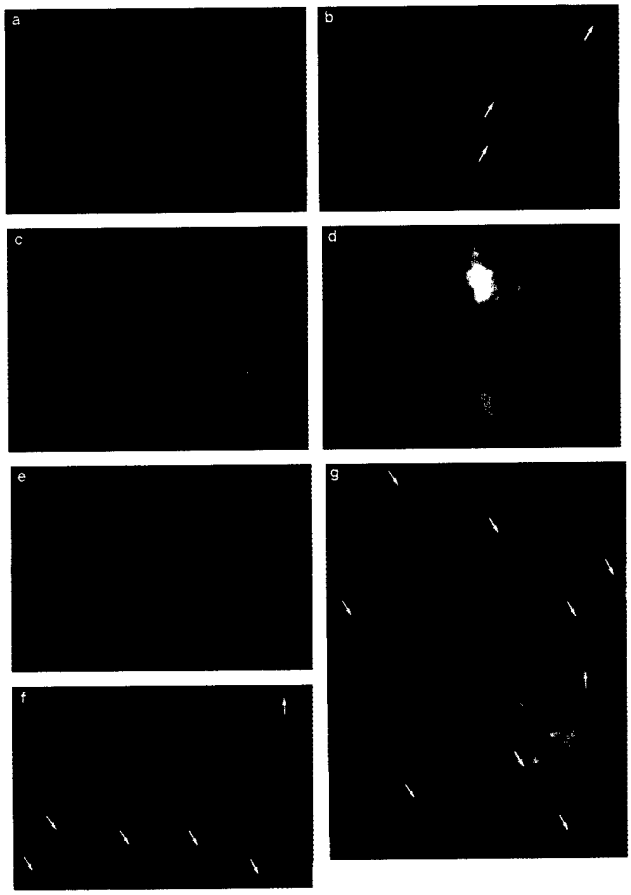

FIG. 3. Morphologic assessment of apoptosis in human glioma cells after γ-irradiation. All cells were stained with DAPI 72 h after being exposed to γ-irradiation. Parental U87MG cells (*a* and *c*) and U87/T691 clonal derivatives (*b* and *d*) are depicted at two magnifications. Nuclei exhibiting apoptotic morphology are indicated by the arrows. Parental U373MG cells (*e*) and U373/T691 subclones 1 (*g*) and 12 (*f*) are shown after staining with DAPI.

(data not shown). Examination of bax and bcl-2 protein levels did not reveal differences between glioblastoma cells and their inhibited subclones.

Apoptosis in p53-Mutated Human Glioblastoma Cells. U373MG human glioma cells contain a mutated p53 gene product, have undetectable levels of the p21 protein (26, 27), and display a comparable elevation of surface EGFR to U87MG cells by flow cytometric analysis. These cells were used to determine whether the observed apoptosis after inhibition of EGFR-mediated signaling and γ-irradiation was dependent on a wild-type p53 protein. U373MG cells exhibited increases in levels of a mutated p53 protein after γ-irradiation but do not express p21 constitutively or after radiation treatment (data not shown, ref. 27).

We expressed the truncated T691stop neu protein in U373MG glioma cells and confirmed expression at levels comparable with U87/T691 cells in four U373/T691 subclones by metabolic labeling and flow cytometic analysis (data not shown). Surface levels for the T691stop neu mutant receptor was equivalent in U87/T691, U373/T691 cl 1 and U373/T691 cl 12 subclones, and two additional T691stop neu-expressing U373MG derivatives. U373/T691 subclones were capable of growth arrest in low serum and displayed a lawn of confluent cells without the development of morphologically transformed foci *in vitro* (data not shown), indicating that wild-type p53 and p21 proteins were not required to arrest growth or inhibit transformation of glioma cells in which erbB signaling was disabled.

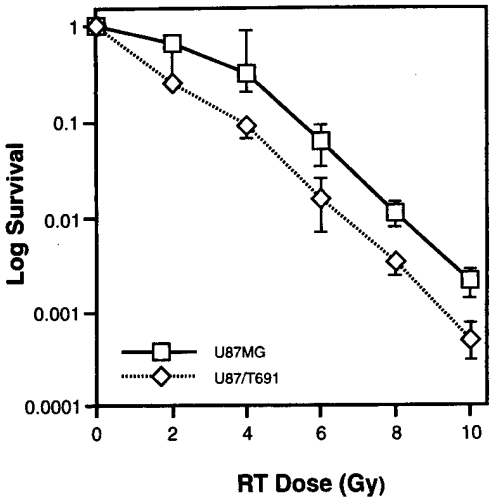

FIG. 4. Clonogenic survival after irradiation. Cells were plated and γ-irradiated with varying doses of radiation followed by incubation for 7–10 days at 37°C with 5% CO_2. Colonies were then stained and those with >50 cells were counted under a dissecting microscope. The log survival was then determined by calculating the ratio of the number of colonies formed to the number of cells plated, after correcting for plating efficiency. Similar experiments were performed three times.

U373/T691 cl 1 and U373/T691 cl 12 subclones exhibited increased levels of apoptosis over parental U373MG cells after radiation (Figs. 2*B* and 3*E-G*). In the representative experiment shown, two U373/T691 subclones exhibited 32% and 59% apoptosis, respectively, 72 h after γ-irradiation, compared with 2% apoptosis in parental U373MG cells and 20% apoptosis in U87/T691 cells. Disabling EGFR signaling by expression of T691stop neu in two distinct human glioma cell lines containing differences in p53 and p21 status resulted in increased radiation-induced apoptosis in each case. Sensitization of human glioblastoma cells to genomic damage can thus occur in the absence of wild-type p53 and p21 proteins. Taken together, these data suggest that both p53-dependent (Fig. 5) and p53-independent pathways may mediate sensitization to cell death induced by a combination of *trans*-receptor inhibition and genomic damage. Of note, human glioblastoma cells in which EGFR signaling is disabled do not appear to be more sensitive to either prolonged serum deprivation or tumor necrosis factor α-mediated cell death than parental cells (data not shown).

DISCUSSION

Specific inhibition of EGFR signaling inhibits cell growth and transformation and also sensitizes radioresistant human glioma cells to radiation-induced genomic damage. Glioblastoma cells expressing a *trans*-dominant p185neu-derived mutant receptor exhibit a greater G_1 phase arrest and higher levels of apoptosis after radiation than their parental counterparts. In

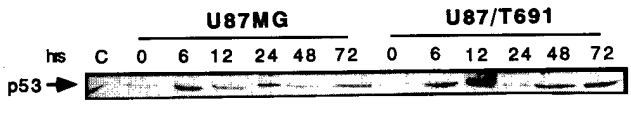

FIG. 5. Analysis of p53 induction in human glioblastoma cells after γ-irradiation. 10^5 U87MG and U87/T691 cells containing a wild-type p53 gene product were plated and γ-irradiated (10 Gy) after attachment overnight. Lysates were then taken at the indicated times after radiation, subjected to SDS/PAGE and immunoblotted with an antibody reactive with p53. Control (C) cells were MCF-7 breast cancer cells containing immunoreactive p53 protein. We consistently demonstrated more robust induction of the p53 protein at 12 h after γ-irradiation in U87/T691 subclones on four independent occasions.

mammalian fibroblasts (28) and in specialized neuronal cells (29, 30), serum or growth factor deprivation can lead to apoptosis under particular conditions. Prolonged serum deprivation alone did not induce apoptosis in human glioblastoma cells in these studies. DNA damage combined with either disabling of erbB receptor signaling or serum deprivation was required to induce apoptosis. Apoptosis was induced by radiation in 23% of U87MG derivatives and in 32–59% of U373MG-derived subclones in which EGFR was disabled (compared with only 1–2% in parental cells) in full growth media, indicating that inhibition of EGFR signaling by *trans*-receptor inhibition could not be overcome by growth in serum. Serum deprivation combined with radiation damage increased observed levels of apoptosis in both parental U87MG cells and T691stop neu-expressing human glioblastoma derivatives to the same degree. Notably, after DNA damage, the apoptosis observed by disabling erbB receptor signaling at the cell surface was greater than that seen with serum deprivation. Counterintuitively, these data also reveal that growth-inhibited glioma cells are more sensitive to radiation-induced cell death. Induction of an inhibitory pathway occurring as a result of EGFR inhibition may thus sensitize cancer cells to radiation-induced growth arrest and/or cell death.

Resistance of γ-irradiated cells is affected by the functional state of distinct oncogenes. Expression of oncogenic Ras or Raf diminishes radiosensitivity in NIH 3T3 cells (31–34) and expression of the Ras^H plus either c- or v-myc oncogenes conferred resistance to rat embryo fibroblasts exposed to γ-irradiation (35). It is also true that expression of various oncogenes can sensitize cells to apoptosis, upon exposure to low serum (28) or to anticancer agents (21, 36). Division delay occurring in both the G_1 and G_2 phases of the cell cycle is influenced by the expression of dominant oncoproteins such as H-ras (17). Expression of a wild-type p53 protein has been associated with decreased survival after γ-irradiation, due to the induction of a higher fraction of apoptosis over cells containing a mutated p53 protein (21, 22). However, tumor cells containing a mutated p53 protein (37) and proliferating lymphoid cells derived from $p53^{-/-}$ mice (38) have been shown to undergo apoptosis after radiation, suggesting p53-independent mechanisms of cell death following genomic damage.

We have shown that p53-dependent mechanisms may influence the response of inhibited glioma cells to undergo relative growth arrest and/or apoptosis. Our results in U373MG-derived cells also indicate that apoptotic cell death occurring after genomic damage in transformed human cells in which EGFR signaling is inhibited involves mechanisms that do not require wild-type p53 and p21 proteins. $p21^{-/-}$ mice develop normally and do not appear to have defects in programmed cell death required for normal organ development, indicating that p21 is not likely to be required for apoptosis (39). $p53^{-/-}$ mice display genetic instability and contain elevated c-myc levels (40). These mice undergo significant levels of apoptosis *in vivo*, indicating that p53-independent mechanisms of apoptosis are functional in both normal tissues (40) and transformed cells (37).

Interestingly, recent work demonstrates that the absence of p21 in isogenically matched colorectal carcinoma cells resulted in reduced growth arrest when compared with p21-positive derivatives of the same cell line and this was correlated to more inhibited tumor growth *in vivo* (3). These observations were ascribed to increased apoptosis due to defects in p21-mediated checkpoint growth arrest, though the increased tendency to apoptose by $p21^{-/-}$ cells was not directly shown in this work. Induction of apoptosis was suggested to be preferable to growth arrest as a response to anticancer therapy *in vivo* (3). In our studies, unlike those of Waldmann *et al.* (3), there was a correlation between apoptosis, increased growth arrest, and reduction in clonogenic survival after radiation. Pathways distal to the specific inhibitory interaction between the T691stop mutant neu protein and the EGF receptor determine tumor responsiveness to genomic damage and these pathways can be modulated by proximal erbB receptor associations. Specific inhibitory pathways initiated at the level of the cell membrane and associated with growth arrest and/or apoptosis may modulate subsequent checkpoint outcomes in response to DNA damage.

Under certain circumstances, particularly in cancer cells, apoptosis may be favored after genomic damage if defects in pathways mediating growth arrest are present (3). Additionally, when cells are capable of undergoing both growth arrest and apoptosis, as in the case of p21-containing and -deficient human glioma cells in which EGFR signaling was disabled in these studies, apoptosis may be induced after certain signals, such as radiation. The ability or inability to induce growth arrest *per se* does not appear to be a major determinant of radiosensitivity because both radioresistant parental human glioblastoma cell lines and more radiosensitive derivatives exhibited growth arrest with prolonged serum deprivation or exposure to radiation, and radiosensitive subclones displayed a greater degree of growth arrest.

Our data indicate that the relative proportion of growth arrest or apoptosis induced by genomic damage is influenced by both the integrity of specific checkpoints and alterations in erbB-signaling pathways. Notably, modulating receptor tyrosine kinase signaling pathways may influence checkpoint outcomes after DNA damage in transformed cells. Others (41) have shown that activation of erbB-signaling pathways in breast cancer cells contributes to radioresistance, suggesting that erbB family-signaling pathways influence the response to DNA damage in many tumor types. By combining biologic inhibition of signaling with agents capable of specifically inhibiting receptor oncoproteins of the tyrosine kinase family, we may be able to influence the kinetics of tumor cell response to standard cytotoxic agents. The timing of administration of cytotoxic therapies may be optimized in such combination therapies ,and these data suggest that selective antitumor effects of presently available anticancer regimens could be improved, even in the treatment of advanced human malignancies containing alterations in multiple checkpoint signal transduction pathways.

This work was supported by a Merit Review Grant from the Veterans Administration (to D.M.O.), by grants from the Lucille P. Markey Trust and the American Association of Neurological Surgeons Research Foundation (to D.M.O.), and by grants from the National Cancer Institute, the National Institutes of Health, the American Cancer Society, the U.S. Army, and the Abramson Institute to M.I.G.

1. Paulovich, A. G., Toczyski, D. P. & Hartwell, L. H. (1997) *Cell* **88,** 315–321.
2. Nurse, P. (1997) *Cell* **91,** 865–867.
3. Waldman, T., Zhang, Y., Dillehay, L., Yu, J., Kinzler, K., Vogelstein, B. & Williams, J. (1997) *Nat. Med.* **3,** 1034–1036.
4. Orren, D. K., Petersen, L. N. & Bohr, V. A. (1997) *Mol. Biol. Cell* **8,** 1129–1142.
5. Louis, D. N. & Gusella, J. F. (1995) *Trends Genet.* **11,** 412–415.
6. Westermark, B. & Nister, M. (1995) *Curr. Opin. Oncol.* **7,** 220–225.
7. Nishikawa, R., Ji, X. D., Harmon, R. C., Lazar, C. S., Gill, G. N., Cavenee, W. K. & Huang, H. J. (1994) *Proc. Natl. Acad. Sci. USA* **91,** 7727–7731.
8. Moscatello, D. K., Montgomery, R. B., Sundareshan, P., McDanel, H., Wong, M. Y. & Wong, A. J. (1996) *Oncogene* **13,** 85–96.
9. O'Rourke, D. M., Nute, E. J. L., Davis, J. G., Wu, C., Lee, A., Murali, R., Zhang, H.-T., Qian, X., Kao, C.-C. & Greene, M. I. (1998) *Oncogene* **16,** 1197–1207.
10. O'Rourke, D. M., Qian, X., Zhang, H.-T., Davis, J. G., Nute, E., Meinkoth, J. & Greene, M. I. (1997) *Proc. Natl. Acad. Sci. USA* **94,** 3250–3255.

11. Prigent, S. A., Nagane, M., Lin, H., Huvar, I., Boss, G. R., Feramisco, J. R., Cavenee, W. K. & Huang, H.-J. S. (1996) *J. Biol. Chem.* **271,** 25639–25645.
12. Moscatello, D. K., Holgado, M. M., Emlet, D. R., Montgomery, R. B. & Wong, A. J. (1998) *J. Biol. Chem.* **273,** 200–206.
13. Holgado-Madruga, M., Moscatello, D. K., Emlet, D. R., Dieterich, R. & Wong, A. J. (1997) *Proc. Natl. Acad. Sci. USA* **94,** 12419–12424.
14. Antonyak, M. A., Moscatello, D. K. & Wong, A. J. (1998) *J. Biol. Chem.* **273,** 2817–2822.
15. Samanta, A., LeVea, C. M., Dougall, W. C., Qian, X. & Greene, M. I. (1994) *Proc. Natl. Acad. Sci. USA* **91,** 1711–1715.
16. Kiyokawa, N., Yan, D. H., Brown, M. E. & Hung, M. C. (1995) *Proc. Natl. Acad. Sci. USA* **92,** 1092–1096.
17. McKenna, W. G., Bernhard, E. J., Markiewicz, D. A., Rudoltz, M. S., Maity, A. & Muschel, R. J. (1996) *Oncogene* **12,** 237–245.
18. Nagane, M., Coufal, F., Lin, H., Bogler, O., Cavenee, W. K. & Huang, H.-J. S. (1996) *Cancer Res.* **56,** 5079–5086.
19. Haas, K. D., Yount, G., Haas, M., Levi, D., Kogan, S. S., Hu, L., Vidair, C., Deen, D. F., Dewey, W. C. & Israel, M. A. (1996) *Int. J. Radiat. Oncol. Biol. Phys.* **36,** 95–103.
20. Lamb, J. R. & Friend, S. H. (1997) *Nat. Med.* **3,** 962–963.
21. Lowe, S. W., Ruley, H. E., Jacks, T. & Housman, D. E. (1993) *Cell* **74,** 957–967.
22. Lowe, S. W., Bodis, S., McClatchey, A., Remington, L., Ruley, H. E., Fisher, D. E., Housman, D. E. & Jacks, T. (1994) *Science* **266,** 807–810.
23. Levine, A. J. (1997) *Cell* **88,** 323–331.
24. Hermeking, H., Lengauer, C., Polyak, K., He, T.-C., Zhang, L., Thiagalingam, S., Kinzler, K. & Vogelstein, B. (1997) *Mol. Cell* **1,** 3–11.
25. Bacus, S. S., Yarden, Y., Oren, M., Chin, D. M., Lyass, L., Zelnick, C. R., Kazarov, A., Toyofuku, W., Gray, B. J., Beerli, R. R., Hynes, N. E., Nikiforov, M., Haffner, R., Gudkov, A. & Keyomarsi, K. (1996) *Oncogene* **12,** 2535–2547.
26. Russell, S. J., Ye, Y. W., Waber, P. G., Shuford, M., Schold, S. J. & Nisen, P. D. (1995) *Cancer* **75,** 1339–1342.
27. Chen, J., Willingham, T., Shuford, M., Bruce, D., Rushing, E., Smith, Y. & Nisen, P. D. (1996) *Oncogene* **13,** 1395–1403.
28. Evan, G. I., Wyllie, A. H., Gilbert, C. S., Littlewood, T. D., Land, H., Brooks, M., Waters, C. M., Penn, L. Z. & Hancock, D. C. (1992) *Cell* **69,** 119–128.
29. Greene, L. A. (1978) *J. Cell Biol.* **78,** 747–755.
30. Batistatou, A. & Greene, L. A. (1993) *J. Cell Biol.* **122,** 523–532.
31. Chang, E. H., Pirollo, K. F., Zou, Z. Q., Cheung, H. Y., Lawler, E. L., Garner, R., White, E., Bernstein, W. B., Fraumeni, J. J. & Blattner, W. A. (1987) *Science* **237,** 1036–1039.
32. Kasid, U., Pfeifer, A., Weichselbaum, R. R., Dritschilo, A. & Mark, G. E. (1987) *Science* **237,** 1039–1041.
33. Kasid, U., Pfeifer, A., Brennan, T., Beckett, M., Weichselbaum, R. R., Dritschilo, A. & Mark, G. E. (1989) *Science* **243,** 1354–1356.
34. Sklar, M. D. (1988) *Science* **239,** 645–647.
35. McKenna, W. G., Weiss, M. C., Endlich, B., Ling, C. C., Bakanauskas, V. J., Kelsten, M. L. & Muschel, R. J. (1990) *Cancer Res.* **50,** 97–102.
36. Harrington, E. A., Fanidi, A. & Evan, G. I. (1994) *Curr. Opin. Genet. Dev.* **4,** 120–129.
37. Bracey, T. S., Miller, J. C., Preece, A. & Paraskeva, C. (1995) *Oncogene* **10,** 2391–2396.
38. Strasser, A., Harris, A. W., Jacks, T. & Cory, S. (1994) *Cell* **79,** 329–339.
39. Deng, C., Zhang, P., Harper, J. W., Elledge, S. J. & Leder, P. (1995) *Cell* **82,** 675–684.
40. Fukasawa, K., Wiener, F., Vande, W. G. & Mai, S. (1997) *Oncogene* **15,** 1295–1302.
41. Wollman, R., Yahalom, J., Maxy, R., Pinto, J. & Fuks, Z. (1994) *Int. J. Radiat. Oncol. Biol. Phys.* **30,** 91–98.

THE JOURNAL OF BIOLOGICAL CHEMISTRY

Vol. 274, No. 2, Issue of January 8, pp. 574–583, 1999
Printed in U.S.A.

Domain-specific Interactions between the p185^{neu} and Epidermal Growth Factor Receptor Kinases Determine Differential Signaling Outcomes*

(Received for publication, March 23, 1998, and in revised form, September 15, 1998)

Xiaolan Qian‡§, Donald M. O'Rourke¶, Zhizhong Fei‡‖, Hong-Tao Zhang‡, Chih-Ching Kao, and Mark I. Greene‡ ‡‡**

*From the ‡Department of Pathology and Laboratory Medicine, and the ¶Department of Neurosurgery, University of Pennsylvania School of Medicine, and the **Department of Pathology, University of Pennsylvania School of Veterinary Medicine, Philadelphia, Pennsylvania 19104*

We expressed the epidermal growth factor receptor (EGFR) along with mutant p185^{neu} proteins containing the rat transmembrane point mutation. The work concerned the study of the contributions made by various p185^{neu} subdomains to signaling induced by a heterodimeric ErbB complex. Co-expression of full-length EGFR and oncogenic p185^{neu} receptors resulted in an increased EGF-induced phosphotyrosine content of p185^{neu}, increased cell proliferation to limiting concentrations of EGF, and increases in both EGF-induced MAPK and phosphatidylinositol 3-kinase (PI 3-kinase) activation. Intracellular domain-deleted p185^{neu} receptors (T691stop neu) were able to associate with full-length EGFR, but induced antagonistic effects on EGF-dependent EGF receptor down-regulation, cell proliferation, and activation of MAPK and PI 3-kinase pathways. Ectodomain-deleted p185^{neu} proteins (TΔ5) were unable to physically associate with EGFR, and extracellular domain-deleted p185^{neu} forms failed to augment activation of MAPK and PI 3-kinase in response to EGF. Association of EGFR with a carboxyl-terminally truncated p185^{neu} mutant (TAPstop) form did not increase transforming efficiency and phosphotyrosine content of the TAPstop species, and proliferation of EGFR·TAPstop-co-expressing cells in response to EGF was similar to cells containing EGFR only. Thus, neither cooperative nor inhibitory effects were observed in cell lines co-expressing either TΔ5 or TAPstop mutant proteins. Unlike the formation of potent homodimer assemblies composed of oncogenic p185^{neu}, the induction of signaling from p185^{neu}·EGFR heteroreceptor assemblies requires the ectodomain for ligand-dependent physical association and intracellular domain contacts for efficient intermolecular kinase activation.

The ErbB family includes four members of homologous receptor tyrosine kinases, the epidermal growth factor receptor (EGFR[1] or ErbB-1) (1), ErbB-2·p185^{neu} (2, 3), ErbB-3 (4), and ErbB-4 (5). ErbB family proteins are widely expressed in epithelial, mesenchymal, and neuronal tissues, and play important roles in normal growth and development (6–9). Aberrant expression of these ErbB proteins is frequently observed in human malignancies (10).

The transmembrane mutation in rat p185^{neu} (also termed Tneu) (12) serves as a paradigm for receptor dimerization that leads to constitutive kinase activation contributing to oncogenic transformation (11–13). Additional support for this mechanism has come from the identification of a naturally occurring activated EGFR oncoprotein (ΔEGFR or EGFRvIII) in human tumors, which forms constitutive dimers and confers increased tumorigenicity (14, 15). Gene amplification and overexpression of ErbB-2 have been observed in a high frequency of human adenocarcinomas, including those of the breast and ovary, and these features correlate with poor clinical prognosis (16, 17). Experimental support for this model is provided by *in vitro* transformation assays using cell lines overexpressing either protooncogenic rat p185$^{c\text{-}neu}$ or human ErbB-2 at levels of 10^6 receptors/cell (18, 19). Biochemical and biophysical analysis of baculovirus-expressed p185^{neu} proteins further support the notion of receptor oligomerization as a mechanism of kinase activation of normal holoreceptors (20, 21).

Heterodimeric interactions govern many signaling properties within the ErbB receptor family. Co-expression of EGFR and p185$^{c\text{-}neu}$ at modestly elevated levels (10^5/cell) (but not either receptor independently) results in synergistic transformation (22), due to increase of the ligand binding affinity and catalytic kinase activity (23, 24). Heterodimerization of EGFR and ErbB-2 has also been observed in human breast tumor lines (25). Moreover, ligand treatment promotes the assembly of an activated p185$^{c\text{-}neu}$·EGFR kinase complex in many cells (24), resulting in novel distinct cellular signaling events (26). Therefore, the receptor tyrosine kinase ensemble can be activated not only by homodimer formation, but also by heterodimeric associations. In this regard, endodomain interactions between p185^{neu} and EGFR appear to influence

* This work was supported by a National Research Service Award (to X. Q.); by grants from the Veterans Administration Merit Review Program, the Lucille Markey Charitable Trust, and the American Cancer Society (IRG-135P) (to D. M. O.); and by grants from National Cancer Institute, the Lucille Markey Charitable Trust, the United States Army, American Cancer Society, and the Abramson Institute for Cancer Research (to M. I. G.). The costs of publication of this article were defrayed in part by the payment of page charges. This article must therefore be hereby marked "*advertisement*" in accordance with 18 U.S.C. Section 1734 solely to indicate this fact.

§ Present address: Laboratory of Cellular Oncology, NCI, National Institutes of Health, Bethesda, MD 20892.

‖ Present address: Cardiology Branch, NHLBI, National Institutes of Health, Bethesda, MD 20892.

‡‡ To whom correspondence should be addressed: 252 John Morgan Bldg., Dept. of Pathology and Laboratory Medicine, 36th and Hamilton Walk, Philadelphia, PA 19104. Tel.: 215-898-2868; Fax: 215-898-2401; E-mail: greene@reo.med.upenn.edu.

[1] The abbreviations used are: EGFR, epidermal growth factor receptor; EGF, epidermal growth factor; PI 3-kinase, phosphatidylinositol 3-kinase; HA, hemagglutinin; PAGE, polyacrylamide gel electrophoresis; MAP, mitogen-activated protein; MAPK, MAP kinase; mAb, monoclonal antibody; aa, amino acid(s); DMEM, Dulbecco's modified Eagle's medium; FBS, fetal bovine serum; PBS, phosphate-buffered saline; MTT, 3,(4,5-dimethylthiazol-2-yl)2,5-diphenyl tetrazolium bromide); ERK, extracellular signal-regulated kinase; BS^3, bis(sulfosuccinimidyl) suberate.

functional signaling outcomes (27).

In response to EGF or Neu differentiating factor/heregulin (a ligand for ErbB-3 and ErbB-4) family ligands (28, 29), EGFR and ErbB-2 both form heterodimers with ErbB-3 and ErbB-4 (30–34). Heterodimers between p185^{neu}·ErbB-2 and ErbB-3 are associated with activated signaling and the transformed phenotype in primary human cancer cells (35). Existence of an ErbB-3·ErbB-4 heterodimer has not been convincingly demonstrated to date. More recent data support the notion that p185^{neu}·ErbB-2 is the preferred heterodimerization partner of *all* ErbB receptors and a mediator for divergent cellular signaling in many distinct cell types (34, 36).

The structural basis for ErbB receptor heterodimerization has not been completely defined and crystallographic information on dimerized ErbB receptor kinases is currently unavailable. Previous work has revealed that ectodomain interactions are sufficient to stabilize dimer formation between p185^{neu} and EGFR in fibroblasts and transformed cells (5, 37, 38), which is supported by observations showing that a partial deletion of the EGF receptor ectodomain still allow dimer formation and receptor activation (14, 15). Although the transmembrane alone can stabilize the formation of p185^{neu} homodimers, the relative contributions of the transmembrane region and the ectodomain have not been directly compared regarding the formation of signaling heterodimers.

In this study, we have constructed various p185^{neu} deletion mutants in order to specifically compare signaling events resulting from associations between EGF receptors and either p185^{neu} ectodomain- or endodomain-derived mutant receptors. We have co-expressed EGFR with *low* levels of p185^{neu} proteins, or their mutant derivatives, to monitor p185^{neu}-mediated enhancement of cell growth and transformation *in vitro* and *in vivo*, and to analyze the influence of EGF-induced heterodimeric receptor interactions on downstream signaling effectors. Signaling resulting from heterodimeric associations between full-length EGFR and mutant p185^{neu} proteins has revealed the functional importance of p185^{neu} subdomains in the induction of Ras/extracellular signal-regulated kinase (ERK) and phosphatidylinositol 3-kinase (PI 3-kinase) pathways contributing to cell growth and transformation.

EXPERIMENTAL PROCEDURES

Antibodies—As described previously (20, 39, 40), monoclonal antibody 7.16.4, polyclonal antiserum α-Bacneu, and NCT are reactive with the ectodomain, intracellular domain, and carboxyl terminus of p185^{neu}, respectively. mAb 225 reactive with the ectodomain of EGFR was obtained from Dr. John Mendelsohn (M. D. Anderson Cancer Center, Dallas, TX). A polyclonal rabbit antiserum specifically against the COOH terminus of EGFR (termed CT) was provided by Dr. Stuart Decker (40). The anti-phosphotyrosine monoclonal antibody, PY20, was obtained from Santa Cruz Biotechnology (Santa Cruz, CA.).

DNA Constructs—All the deletion mutants were derived from the rat oncogenic p185^{neu} cDNA containing a single point mutation (V664G) in the transmembrane region. The TAPstop mutant, containing a 122-aa truncation of the COOH terminus was prepared as described previously (41). A T691stop species was prepared by site-directed mutagenesis and substitution of a stop codon for Thr-691, resulting in a large cytoplasmic deletion (42, 43). The ectodomain-deleted mutant TΔ5 neu protein was described previously (27). These cDNAs encoding for mutant p185^{neu} forms were all cloned into the pSV2neo^{r}/DHFR vector as described (44) for expression in murine fibroblasts. These wild-type or mutant p185^{neu} cDNAs were also subcloned into pcDNA3 vector for transient expression in COS7 cells. pSRαEGFR/hyg^{r} vector (44) was used for full-length EGFR expression.

Transfection and Maintenance of Cell Lines—Ten micrograms of the p185^{neu} constructs were transfected into NR6 cells, a mouse fibroblast cell line devoid of endogenous EGF receptors (43), or NE91 cells expressing human EGFR (37) by calcium phosphate precipitation. After 2–3 weeks of selection with Geneticin (0.9 mg/ml), the established stable clones were screened and characterized. Gene amplification by methotrexate was used to increase the p185^{neu} receptor level. Expression of p185^{neu} and its derivatives in resultant subclones was examined by flow cytometric analysis following anti-p185^{neu} mAb 7.16.4 staining. Surface expression of p185^{neu} proteins was then estimated by comparing the mean channel fluorescent intensity with that of B104-1-1 cells, as the level of p185^{neu} in B104-1-1 cells was previously determined by ^{125}I-labeled anti-neu mAb binding assay (22). EGFR numbers in NE91 cells and mutant p185^{neu} co-transfected cells were determined by Scatchard assays as described (37). These transfected clones were maintained in Dulbecco's modified Eagle's medium (DMEM) containing 5% fetal bovine serum (FBS, HyClone) at 37 °C in a 5% CO_2 atmosphere.

Cross-linking, Immunoprecipitation, and Immunoblotting Procedures—Subconfluent cells in 10-cm dishes were washed and starved in cysteine-free DMEM for 1 h, and grown in low cysteine-containing 5% FBS-DMEM containing 55 μCi/ml [^{35}S]cysteine (Amersham Pharmacia Biotech) for 16 h for metabolic labeling. Alternatively, the unlabeled cells were cultured overnight in 10-cm Petri dishes. After treatment with or without EGF, cells were washed twice with cold phosphate-buffered saline (PBS) and treated with PBS containing 2 mM membrane-impermeable cross-linker bis(sulfosuccinimidyl) suberate (BS^{3}, Pierce), for 30 min. After quenching the cross-linking reaction with a buffer containing 10 mM Tris-HCl (pH 7.6), 0.9% NaCl, and 0.1 M glycine, cells were washed twice with cold PBS and solubilized with PI/RIPA buffer as described (24). The immunocomplexes were washed and solubilized, then separated by gradient SDS-PAGE gels (4–7.5%). Proteins from metabolically labeled cells were analyzed by autoradiography. Proteins from unlabeled cells were transferred onto nitrocellulose and then immunoblotted with anti-phosphotyrosine mAb PY20, anti-EGFR CT, or anti-p185 antiserum as indicated in the figures. The protein signals were identified by the binding of ^{125}I-labeled protein A (NEN Life Science Products), or by enhanced chemiluminase (ECL) using ECL kit from Amersham Pharmacia Biotech.

Receptor Down-regulation Studies—Cells (1×10^5) were plated in a six-well dish with DMEM containing 5% FBS overnight. Cells were then treated with EGF (50 ng/ml) for 0–4 h and were harvested and washed with cold PBS containing 0.5% bovine serum albumin and 0.1% sodium azide. Cell preparations were then incubated with a saturating amount (0.5 μg/reaction) of anti-neu mAb 7.16.4 or anti-EGFR mAb 225, or an irrelevant mAB (such as 9BG5 against the hemagglutinin of reovirus receptor), at 4 °C for 30 min, restained with fluorescein isothiocyanate-conjugated anti-mouse IgG (Sigma) for another 30 min after extensive washing. Cells were then fixed with 2% paraformaldehyde and analyzed by flow cytometry (FACScan, Becton Dickinson), as described previously (37). Briefly, after subtracting the nonspecific background staining with 9BG5, the mean channel values from each time point were used to determine the percentage of surface expression of EGFR or p185^{neu} proteins at the various time points after EGF treatment.

In Vitro and in Vivo Transformation Assays—Anchorage-independent growth ability was determined by assessing the colony forming efficiency of cells suspended in soft agar (15, 37). Cells (1000/dish) were suspended in 7% FBS-DMEM containing 0.18% agarose, and plated on 0.25% basal agar in each dish. Cells were fed with DMEM supplemented with 7% FBS-DMEM, 20 mM HEPES (pH 7.5). Colonies (>0.3 mm) were visualized at day 21 for all cell lines after stained with *p*-iodonitrotetrazolium violet (1 mg/ml). Each cell line was examined in triplicate samples for separate experiments.

To analyze the tumor growth in athymic mice, cells (1×10^6) of each line were suspended in 0.1 ml of PBS and injected intradermally in the mid-dorsum of NCR nude mice. PBS alone was also injected as a control. Animals used in this study were maintained in accordance with the guidelines of the Committee on Animals of the University of Pennsylvania and those prepared by the Committee on Care and Use of Laboratory Animals of the Institute of Laboratory Animal Resource. Tumor growth was monitored twice a week up to 10 weeks. Tumor size was calculated by this formula: 3.14/6 × (length × width × thickness) as described (27).

EGF-dependent Cell Proliferation Assay—The 3,(4,5-dimethylthiazol-2-yl)2,5-diphenyl tetrazolium bromide) (MTT) assay for measuring cell growth has been described previously (38). Briefly, cells (3000/well) of each cell line were seeded in 96-well plates overnight in DMEM containing 5% FBS. Cells were starved in serum-free ITS-DMEM for 48 h, then cultured in 100 μl of the same medium plus various concentrations of EGF for another 48 h. 25 μl of MTT solution (5 μg/ml in PBS) were added to each well, and after 2 h of incubation at 37 °C, 100 μl of the extraction buffer (20% w/v SDS, 50% *N,N*-dimethyl formamide, pH 4.7) was added. After an overnight incubation at 37 °C, the optical density at 600 nm was measured using an enzyme-linked immunosorbent assay reader. Each value represents a mean of four samples.

MAP Kinase and PI 3-Kinase Immune Complex Kinase Assays—COS7 cells were transiently transfected with pcDNA3-HA-ERK2 (a gift from Silvio Gutkind, National Institutes of Health, Bethesda, MD) and pSRαEGFR/hyg^r, along with either empty vector or plasmids expressing wild-type or mutant p185$^{c\text{-}neu}$ using LipofectAMINE (Life Technologies, Inc.) according to the manufacturer's instructions and assayed 48 h after transfection. Cells deprived of serum for 16–20 h were treated with or without EGF (50 ng/ml) for 5 min. For MAP kinase assay, cells were lysed with RIPA buffer (25 mM Tris-HCl (pH 7.5), 0.3 M NaCl, 1.5 mM $MgCl_2$, 1 mM $MgCl_2$, 0.2 mM EDTA, 0.5 mM dithiothreitol, 1% Triton X-100, 0.5% sodium deoxycholate, 0.1% SDS, 20 mM β-glycerophosphate, 1 mM sodium orthovanadate, 10 μg/ml aprotinin, 1 mM phenylmethylsulfonyl fluoride, 10 μg/ml leupeptin). Protein concentrations were determined by the BCA kit (Pierce). Equal amounts of protein (100 μg) from cell extracts were immunoprecipitated with anti-HA (BabCo). After washing extensively, the immunocomplexes were then incubated with 50 μl of reaction buffer (30 mM HEPES (pH 7.4), 10 mM $MaCl_2$, 1 mM dithiothreitol, 5 μM ATP) containing 1 μCi of [γ-^{32}P]ATP (NEN Life Science Products) and 2 μg of myelin basic protein (Upstate Biotechnology Inc.). After incubation for 20 min at 30 °C, kinase reactions were terminated by the addition of 2× Laemmli sample buffer. The samples were then resolved by SDS-PAGE, and the phosphorylated myelin basic protein was visualized by autoradiography.

PI 3-kinase immune complex assays were carried out as described (45) with slight modifications. Cells were lysed in Nonidet P-40 lysis buffer (20 mM Tris-HCl (pH 7.4), 137 mM NaCl, 1 mM $MgCl_2$, 1 mM $CaCl_2$, 10% glycerol, 1% Nonidet P-40, 1 mM sodium orthovanadate, 10 μg/ml aprotinin, 1 mM phenylmethylsulfonyl fluoride, 1 μg/ml leupeptin). Equal amounts of protein (600 μg) from cell extracts were immunoprecipitated with anti-phosphotyrosine 4G10 (Upstate Biotechnology Inc.) for 3 h. Protein A-Sepharose was then added and rotated at 4 °C for overnight. Immunocomplexes were washed twice with lysis buffer; twice with 100 mM Tris (pH 7.4), 0.5 M LiCl, 0.2 mM sodium orthovanadate, plus 0.2 mM adenosine; and twice with reaction buffer (10 mM HEPES (pH 7.5), 5 mM EDTA, 150 mM NaCl). The beads were resuspended in 40 μl of reaction buffer containing substrate mixture (phosphatidylinositol, phosphatidylinositol 4-phosphate, and phosphatidylserine dispersed by sonication in 10 mM HEPES (pH 7.5), 1 mM EGTA). The tubes were incubated at room temperature for 10 min and reaction were initiated by adding 5 μCi of [γ-^{32}P]ATP (NEN Life Science Products) per reaction in 5 μl of 500 mM ATP and terminated by addition of 80 μl of $CHCl_3$:CH_3OH (1:1) after another 10 min. Phospholipids were extracted, desiccated, and redissolved as described (45). The samples were the chromatographed on thin layer chromatography plates (precoated with potassium oxalate and baked at 100 °C for 1 h before use) in $CHCl_3$:CHOH:2.5 M NH_4OH:H_2O (45:35:2.7:7.3). Spots corresponding to phosphatidylinositol 3-phosphate and phosphatidylinositol 3,4-bisphosphate were visualized after autoradiography. Unlabeled phospholipid standards were included and were visualized by exposure to iodine vapor.

RESULTS

Expression of EGFR and/or Mutant p185^{neu} Proteins—Cell lines expressing EGFR and various p185^{neu} deletion mutant proteins derived from full-length transforming p185^{neu} were all generated in the NR6 cell background (43). In addition, stable transfectants derived from NR6 fibroblasts expressing human EGFR (termed NE91 cells) were also generated. NE91 cells, as well as NR6 parental cells, were then transfected with various p185^{neu} cDNA constructs to express one of the following mutant p185^{neu} proteins with or without EGFR, respectively (Fig. 1): (*a*) Er/p185^{neu} or p185^{neu} (full-length oncogenic p185^{neu} product), (*b*) Er/T691stop or T691stop (lacking 591 aa from the carboxyl terminus), (*c*) Er/TAPstop or TAPstop (a 122-aa truncation at carboxyl terminus), and (*d*) Er/TΔ5 or TΔ5 (an ectodomain deleted p185^{neu} product, also termed TΔ5). A schematic representation of the oncogenic p185^{neu} protein and its mutant derivative species is shown in Fig. 1.

B104-1-1 murine fibroblasts transformed by the expression of oncogenic p185^{neu} were used as a positive control, since surface expression of p185^{neu}, biochemical features of p185^{neu} homodimerization and p185^{neu} transforming potency have been characterized previously (13, 22, 27). As shown in Table I, relative expression levels of various p185^{neu} mutant proteins in

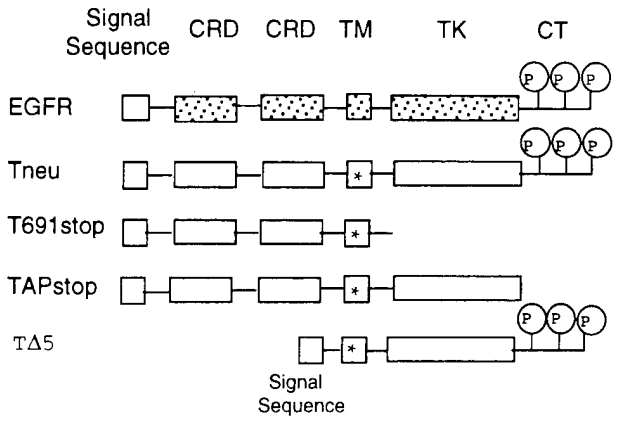

FIG. 1. **Schematic representation of EGFR and mutant p185^{neu} proteins.** Locations of cysteine-rich subdomains (*CRD*), transmembrane region (*TM*) containing the point mutation V664E (*), tyrosine kinase domain (*TK*), and carboxyl-terminal region (*CT*) are indicated. *Tneu* is the full-length transforming rat p185^{neu}. *T691stop* contains a stop codon substituting for Thr-691 at the amino terminus to the TK domain. *TAPstop* contains a 120-aa truncation within the carboxyl terminus of p185^{neu}. *TΔ5* is generated by the deletion of ectodomain of p185^{neu} but retains ~10 aa and the signal sequence. These mutant p185^{neu} proteins were either expressed alone or co-expressed with EGFR in NR6 transfected cells.

selected clones were estimated by a comparison with B104-1-1 cells, while the expression of EGFR in these cells was estimated by Scatchard analysis. In order to observe an enhancement of EGFR-mediated cellular signaling and transformation, clone Er/p185^{neu} expressing a moderately low level of both receptors (~10^4/cell) was chosen. In other subclones, the expression of EGFR and/or mutant p185^{neu} proteins was approximately ~10^5 receptors/cell.

The Ectodomain of p185^{neu} Is Required for Heterodimerization with EGFR—Stable cell lines expressing EGFR and/or mutant p185^{neu} proteins were used to assess dimer formation using the chemical cross-linker BS^3. As shown in Fig. 2, B104-1-1 cells expressing oncogenic p185^{neu} contained p185^{neu} homodimers (~370 kDa) independent of ligand stimulation (Fig. 2*A*, *lane 1*), due to the activating transmembrane mutation (12). A cell line expressing the ectodomain-derived T691stop neu alone was used as a control to demonstrate the sizes of the monomer and dimer of this truncated p185^{neu} protein, which migrated at approximately 115 kDa (Fig. 2*A*, *lanes 2* and *3*), and at ~230 kDa in the presence of a chemical cross-linker (Fig. 2*A*, *lane 3*).

In the presence of EGF, the 170-kDa monomeric form and the 340-kDa homodimer of EGFR were both detected in NE91 cells expressing EGFR alone, and in Er/T691stop cells (Fig. 2*A*, *lanes 4* and *5*, respectively). An additional intermediate band of ~285 kDa representing the heterodimer of EGFR and T691stop was clearly detectable upon anti-EGFR immunoprecipitation (Fig. 2*A*, *lane 5*). The 285-kDa intermediate complex was similar to the heterodimer composed of EGFR and truncated N691stop derived from proto-oncogenic p185$^{c\text{-}neu}$ as described previously (44), except that the heterodimeric EGFR·N691stop complex was even more predominant than the EGFR homodimer in those studies. Notably, T691stop is still able to complex with EGFR (*lane 5*) even under conditions favorable for T691stop homodimerization (*lane 3*). Densitometric analysis suggested that at least 50% of the EGFR associated with T691stop neu in a heterodimeric complex in Er/T691stop cells (Fig. 2*A*, *lane 5*), further suggesting the strong preference for EGFR·p185^{neu} heterodimerization.

We have previously studied complex formation between the p185^{neu} and EGFR holoreceptors (22, 24, 37) and heterodimer-

TABLE I

Transformation parameters and relative receptor expression levels of cell lines

The number of EGFR on NE91 and other transfected cells was determined by Scatchard assays. Cell surface expression of neu proteins were estimated by comparing the mean channel fluorescent intensity with that from B104–1-1 cells using flow cytometry analysis. $p185^{neu}$ on B104–1-1 cells was originally determined by an ^{125}I-labeled anti-neu mAb binding assay (22). For the tumor growth assay, individual clones (1×10^6 cells/site) were injected intradermally into athymic mice. NT, no tumor after 10 weeks; ND, not determined.

Cells	Colony in soft agar	Tumor growth			Receptor expression	
		Incidence	Latency	mm^3 (at week 6)	Neu protein	EGFR
	% efficiency		*week*			
B104–1-1	33.7 ± 0.6	6/6	1	sacrificed	1.5×10^5	0
NE91	<0.1	0/4		NT	0	2.8×10^5
Tneu	5.4 ± 0.4	4/4	4–5	158.5	3.7×10^4	0
Er/neu	10.2 ± 0.6	6/6	2–2.5	663	3.9×10^4	3.8×10^4
T691stop	<0.1	0/4		NT	4.5×10^5	0
Er/T691stop	<0.1	0/4		NT	4.3×10^5	2.5×10^5
TAPstop	6.5 ± 0.5	6/6	4–5	177.6	1.2×10^5	0
Er/TAP/stop	5.5 ± 0.6	4/4	4–5	168.7	1.3×10^5	4.6×10^5
TΔ5	5.7 ± 0.3	6/6	3	545.7	ND	0
Er/TΔ5	6.6 ± 0.4	4/4	3	593.4	ND	1.6×10^5

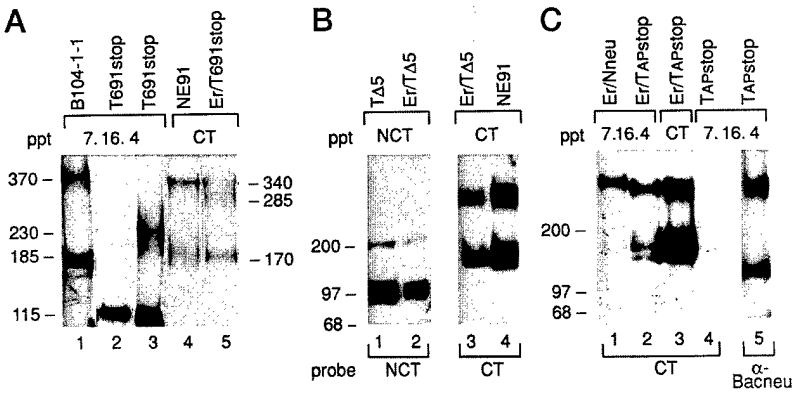

FIG. 2. **Homodimerization and heterodimerization of EGFR and $p185^{neu}$ proteins.** *A*, cells were labeled with [^{35}S]cysteine overnight. Cell lines expressing EGFR (*lanes 4* and *5*) were then stimulated with EGF (200 ng/ml) at 37 °C for 10 min. All cells (except *lane 2*) were treated with the chemical cross-linker BS^3 (2 mM). Cell lysates were then immunoprecipitated with anti-neu mAb 7.16.4 or anti-EGFR antiserum CT as indicated. Proteins were separated by 4–8% gradient SDS-PAGE and analyzed by autoradiography. The estimated molecular weight of monomers and dimers is indicated. *B* and *C*, cell lines expressing EGFR (NE91, Er/TΔ5, and Er/TAPstop) were stimulated with EGF. After BS^3 treatment, all the cells were lysed and subjected to immunoprecipitation with either anti-neu (7.16.4 or NCT) or anti-EGFR (CT) antibodies, then immunoblotted with either the anti-neu (NCT or α-Bacneu) or anti-EGFR probe (CT) as indicated.

ization between ectodomain $p185^{neu}$ and either full-length (37, 44) EGFR or a form of EGFR that lacks the majority of subdomains 1 and 2 (15) by immunoprecipitation and immunoblotting using anti-receptor specific antibodies following EGF and chemical cross-linker treatment.

In this next set of studies, we extended these observations to novel species of $p185^{neu}$. Er/Nneu cells expressing higher levels of EGFR and normal $p185^{c\text{-}neu}$ served as a positive control to examine the physical association of EGFR with truncated mutant $p185^{neu}$ receptor forms (Fig. 2*C*, *lane 1*). The heterodimer between full-length $p185^{neu}$ with EGFR in Er/neu cells could not be detected due to low expression levels of each receptor (data not shown). Abundant levels of the EGFR monomer and dimer were detected in Er/TAPstop cells by anti-EGFR immunoprecipitation and immunoblotting (Fig. 2*C*, *lane 3*). Analysis of anti-$p185^{neu}$ immunoprecipitates by immunoblotting with anti-EGFR antisera indicated EGF-induced heterodimerization of EGFR and TAPstop in Er/TAPstop cells (Fig. 2*C*, *lane 2*). As expected, the size of this complex was slightly smaller when compared with the heterodimer of EGFR and full-length normal $p185^{neu}$ in Er/Nneu cells (Fig. 2*C*, *lane 1*). The control cell line expressing TAPstop alone showed that TAPstop was only recognized by an anti-neu antibody (Fig. 2*C*, *lane 5*), but not by anti-EGFR antibody CT (Fig. 2*C*, *lane 4*).

Heterodimerization between EGFR and the ectodomain-deleted TΔ5 $p185^{neu}$ mutant was also analyzed. TΔ5 can be recognized by either the α-Bacneu or anti-NCT polyclonal antisera reactive with the intracellular domain or carboxyl terminus of the $p185^{neu}$ protein, respectively. Immunoblotting showed that the size of the TΔ5 neu mutant was approximately 95–97 kDa, and the detectable dimeric form was about ~200 kDa (Fig. 2*B*, *lane 1*). Er/TΔ5 cells express a high level of EGFR and TΔ5, as homodimers of either form were clearly detected in the presence of cross-linker (Fig. 2*B*, *lanes 2* and *3*), when compared with control cell lines NE91 and TΔ5 (Fig. 2*B*, *lanes 1* and *4*). However, unlike Er/T691stop and Er/TAPstop cells, the heterodimer between EGFR and TΔ5 in Er/TΔ5 cells was undetectable following EGF and BS^3 treatment since the predicted intermediate size (~270 kDa) complex representing EGFR and TΔ5 heterodimer was not observed (Fig. 2*B*, *lanes 2* and *3*). In an attempt to identify the association of EGFR with this ectodomain-deleted TΔ5 protein, several alternative assays were performed, such as using the membrane-permeable chemical cross-linker DSP (Pierce), or a mild detergent digitonin lysis buffer. These methods were sensitive enough to detect the complex formation between full-length $p185^{neu}$ and TΔ5 (27).

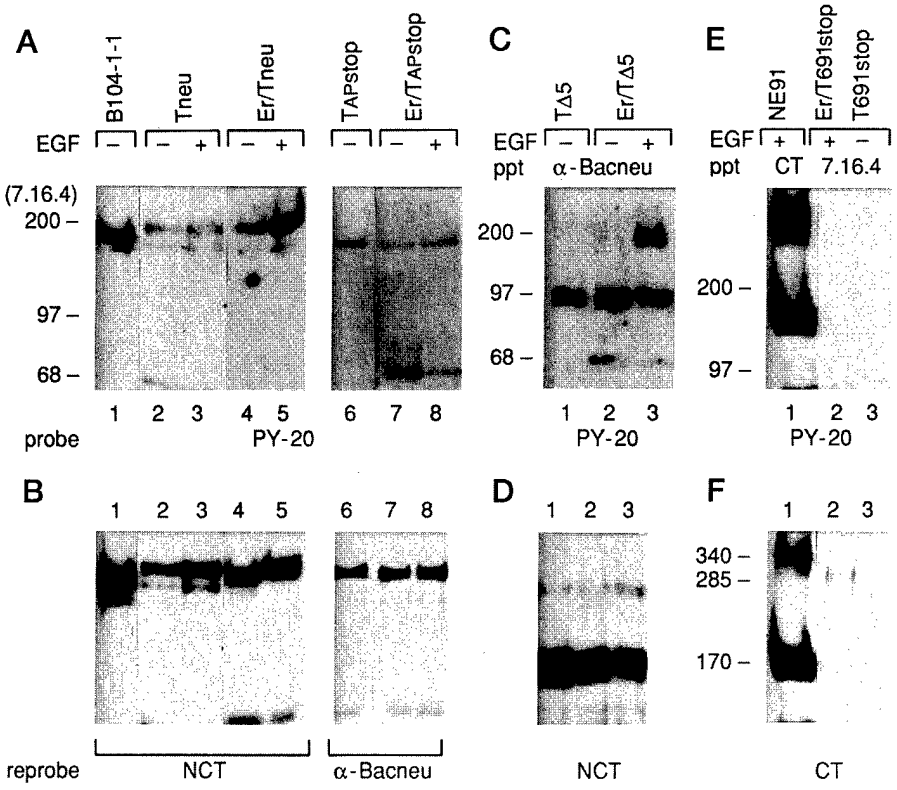

FIG. 3. **Tyrosine phosphorylation of EGFR and mutant p185^{neu} proteins in living cells.** Cells in *panels A, C,* and *E* were treated with or without EGF as indicated. Cells in *panel E* were also treated with the chemical cross-linker BS^3 (2 mM). Cell lysates were then immunoprecipitated with anti-neu antibodies, 7.16.4, α-Bacneu, or anti-EGFR CT as indicated. Proteins were separated by 6% (*A* and *C*) or 4–8% (*E*) gradient SDS-PAGE followed by immunoblotting with anti-phosphotyrosine mAb PY-20. After stripping the PY20 signals presented in *top panels*, these nitrocellulose membranes were reprobed with anti-neu NCT (*B, lanes 1–5,* and *D*), α-Bacneu (*B, lanes 6–8*) or α-EGFR CT (*F*) to compare protein amounts used in each sample.

However, the association of EGFR and TΔ5 was still undetectable (data not shown). Taken together, these results strongly suggest that the ectodomain of the p185^{neu} receptor is necessary and sufficient for heterodimerization with holoreceptor EGFR.

Tyrosine Kinase Activity in Living Cells—It has been well documented that EGF, in an EGFR-dependent manner, stimulated phosphorylation of the p185$^{c\text{-}neu}$ and c-ErbB-2 gene products with a concomitant increase in their tyrosine kinase activities (46–49). Heterodimerization of p185 and EGFR facilitates cross-phosphorylation (24, 25), since a full-length, kinase-deficient p185^{neu} mutant (K757M) is trans-phosphorylated upon physical association with EGFR (37). We next examined the tyrosine phosphorylation level of p185^{neu} derivatives in living cells in response to EGF treatment. After the addition of EGF, oncogenic p185^{neu} and its derivatives were immunoprecipitated by anti-neu antibodies, and receptor phosphotyrosine content *in vivo* was detected by immunoblotting with an anti-phosphotyrosine antibody (PY20) (Fig. 3). Full-length p185^{neu} from control B104-1-1 fibroblasts displayed constitutive kinase activity (Fig. 3*A, lane 1*). Upon EGF stimulation, there was indeed an additional increase in tyrosine kinase activity of p185^{neu} in Er/neu cells expressing lower amounts of the p185^{neu} protein (Fig. 3*A, lanes 4* and *5*), but not in cells expressing p185^{neu} alone (*lanes 2* and *3*). A weak tyrosine phosphorylation signal was detected in TAPstop cells (Fig. 3*A, lane 6*). EGF stimulation did not appreciably increase the tyrosine phosphorylation of TAPstop in EGFR-co-expressing cells (Fig. 3*A, lanes 7* and *8*), although the association of EGFR and TAPstop was evident (Fig. 2*C*). Truncation of the p185^{neu} carboxyl terminus, and deletion of at least three known critical tyrosine residues, was associated with the failure to trans-phosphorylate the p185^{neu} mutant protein. Elimination of the ectodomain did not impair the intrinsic kinase activity of p185^{neu}-derived TΔ5, since the TΔ5 mutant receptor was still a competent tyrosine kinase (Fig. 3*C, lane 1*). However, unlike the full-length p185^{neu}, no further increase in tyrosine phosphorylation of TΔ5 was detected in Er/TΔ5 cells with EGF stimulation (Fig. 3*C, lane 2* and *3*). In Er/TΔ5 cells, the EGFR was also immunoprecipitated by the anti-Bacneu antisera and still autophosphorylated after EGF treatment (Fig. 3*C, lane 3*). These results correlated with failure to detect physical interactions between EGFR and TΔ5 proteins (Fig. 2). Reprobing with anti-neu antibodies (Fig. 3, *A* and *C*) confirmed equivalent protein loading in paired samples with or without EGF treatment (Fig. 3, *B* and *D*). These experiments indicated that the full-length p185^{neu} receptor, but not mutant p185^{neu} proteins with NH_2-terminal or distal COOH-terminal truncations, was able to interact with activated EGFR functionally, resulting in trans-phosphorylation.

We next analyzed tyrosine kinase activation in EGFR-positive NE91 cells with or without T691stop neu co-expression. Treatment with EGF and a chemical cross-linking reagent resulted in heavy tyrosine phosphorylation of EGFR monomers and homodimers in NE91 cells (Fig. 3*E, lane 1*). No detectable tyrosine phosphorylation of cytoplasmic domain-deleted T691stop neu was seen in cells with or without EGFR co-expression (Fig. 3*E, lanes 2* and *3*, respectively). In addition, the tyrosine phosphorylation signal of an intermediate band (~285 kDa) representing EGFR·T691stop heterodimeric complex was also undetectable (Fig. 3*E, lane 2*), although a significant portion of EGFR forms a heterodimer with T691stop under these conditions (Fig. 2*A, lane 5*). Tyrosine kinase activation of full-length EGFR was thus completely inhibited when EGFR was physically associated with the T691stop neu mutant protein, which correlates with reduction of the transformed phenotype of primary EGFR-positive glioma cells expressing T691stop neu (42). Moreover, these results are consistent with the observation from cells co-expressing EGFR with N691stop neu derived from normal p185^{neu} (37).

Re-probing the membrane with an anti-EGFR antibody (CT) showed total EGFR levels in NE91 cells (Fig. 3*F, lane 1*), and confirmed the presence of the EGFR·T691stop heterodimer (~285 kDa), since this complex was recognized by anti-neu in

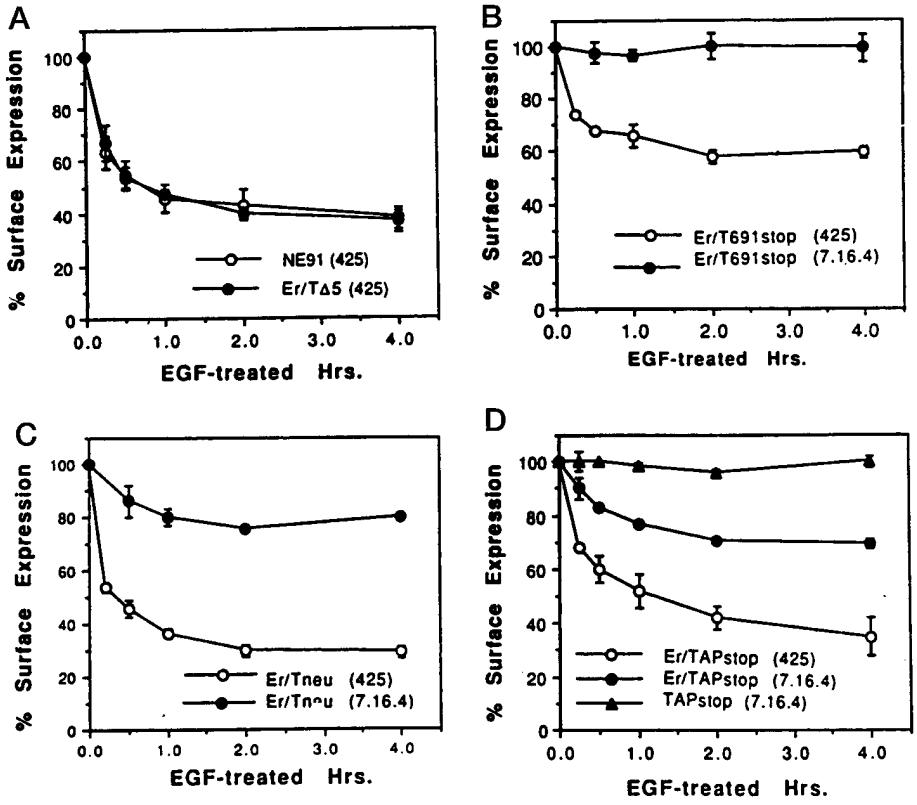

FIG. 4. **EGF-mediated receptor down-regulation.** Cells were plated in six-well dishes overnight and treated with EGF (50 ng/ml) for 0–4 h at 37 °C. Cells were then washed with fluorescence-activated cell sorting buffer and stained with anti-neu mAb 7.16.4 or anti-EGFR mAb 425 as indicated. After subtracting the background staining with irrelevant mAb 9BG5, the percentage of cell surface receptor expression reflected by the mean fluorescent intensity from each treated sample verses that from a non-treated sample was plotted against EGF treatment time. *A*, NE91 and Er/TΔ5; *B*, Er/T691stop; *C*, Er/neu; *D*, TAPstop and Er/TAPstop.

immunoprecipitation and anti-EGFR in immunoblotting (Fig. 3*F*, *lane 2*). Lysates obtained from T691stop neu-expressing cells did not react with the anti-EGFR CT probe (Fig. 3*F*, *lane 3*). Although the cytoplasmic domain deletion in T691stop did not impair heterodimerization with EGFR, the undetectable phosphotyrosine content of the intermediate heterodimer suggested that EGFR kinase activity was reduced when associated with T691stop neu. These experiments further support our model that the heteroreceptor assembly mediated primarily by ectodomain interactions facilitates kinase trans-activation and trans-phosphorylation caused by interactions between cytoplasmic domains (15, 27, 37).

EGF-induced Receptor Down-regulation from the Cell Surface—Numerous studies indicate that ligand-mediated receptor endocytosis and degradation is a kinase-dependent process for many types of growth factor receptors (50). We found that the efficiency of receptor down-regulation and degradation in cells co-expressing EGFR and p185^{neu} correlated well with heterodimeric kinase activities (37). We used this method as an alternative assay to examine the kinase activity of various heterodimers.

Cells were incubated with EGF (50 ng/ml) for various times prior to cell surface staining with anti-neu mAb 7.16.4 or anti-EGFR mAb 225 followed by the staining with fluorescein isothiocyanate-conjugated anti-mouse-IgG. Cell surface expression of each receptor was analyzed using flow cytometric analysis. EGF treatment of NE91 cells (expressing EGFR only) resulted in a reduction of cell surface EGFR, and over 60% of EGF receptors disappeared from the cell surface after 4 h of treatment (Fig. 4*A*). Normal EGFR down-regulation was not affected by the co-expression of TΔ5, as the efficiency of EGFR down-regulation in Er/TΔ5 cells was very similar to that seen in NE91 cells (Fig. 4*A*). A similar EGFR down-regulation curve was observed in Er/neu and Er/TAPstop cells (Fig. 4, *C* and *D*, respectively), indicating that the EGFR behaves as an active receptor kinase in these cells. Moreover, about ~20% of p185^{neu} or 25% TAPstop was co-down-regulated with EGFR upon EGF stimulation (Fig. 4, *C* and *D*). As illustrated above, the low expression of p185^{neu} and EGFR in Er/neu cells was insufficient to demonstrate the physical association of the two receptors biochemically. The current assay was more sensitive in determining EGF-mediated receptor interactions. Control cells expressing TAPstop alone did not respond to EGF treatment, and the surface expression of TAPstop remained unchanged within the period of EGF treatment (Fig. 4*D*).

Analysis using an EGF-mediated pulse-chase assay showed that the down-regulated EGFR and co-down-regulated TAPstop proteins efficiently went into the degradation pathway (data not shown), similar to the cells overexpressing EGFR and p185^{neu} (37). Our data suggested that EGFR and either p185^{neu} or TAPstop associated into an active kinase complex and that these receptor assemblies exhibited comparable kinetics of receptor endocytosis.

However, co-expression of T691stop with EGFR resulted in diminished EGF-induced down-regulation of EGFR. The maximal reduction of surface EGF receptor was ~35% after 4 h. In addition, no detectable co-down-regulation of the cytoplasmic domain deleted T691stop was observed in Er/T691stop cells (Fig. 4*B*), correlating with the observation of the inactive heterodimer of EGFR·T691stop (Fig. 3, *E* and *F*). This finding supports the idea that receptor down-regulation is coupled to receptor tyrosine kinase activity. The formation of the inactive heterodimer between EGFR and T691stop neu proteins influenced the overall kinetics of EGFR down-regulation. Impairment of ligand-induced down-regulation of holo-EGFR by T691stop neu has also been observed in primary human cancer cells.[2]

Transforming Potency of Cells Expressing Mutant p185^{neu} Proteins with or without EGFR—We and others have showed that the transforming potency of p185^{neu} requires not only its intrinsic tyrosine kinase activity (13), but also the crucial role

[2] D. M. O'Rourke and M. I. Greene, unpublished observations.

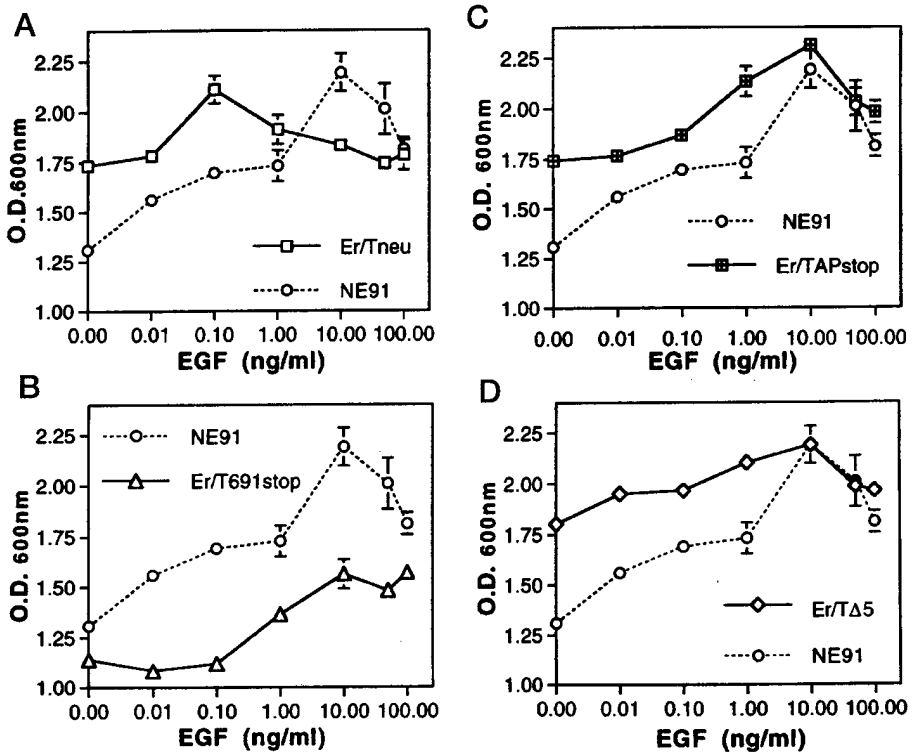

FIG. 5. **EGF-induced cell proliferation.** Cells were plated in 96-well plates (3000/well) overnight in DMEM containing 5% FBS. After starvation in serum-free media for 48 h, cells were grown in the same media supplemented with various concentrations of EGF as indicated for an additional 48-h period. Cell proliferation was determined by the MTT assay as described under "Experimental Procedures." The resultant OD_{600} was plotted against the relevant EGF concentration. NE91 cells was used as a control for the cell lines presented: *A*, Er/neu; *B*, Er/T691stop; *C*, Er/TAPstop; *D*, Er/TΔ5.

of tyrosine phosphorylation of its carboxyl terminus, as the oncogenicity of $p185^{neu}$ was greatly reduced by alteration of several tyrosine residues (41) or large structural deletions, such as seen with TAPstop (42). Transforming ability of ectodomain-deleted TΔ5 in this system was less potent than full-length $p185^{neu}$, possibly due to the reduced efficiency of forming active receptor complexes when compared with full-length oncogenic $p185^{neu}$ (27) (see Fig. 2).

We examined whether co-expression of EGFR with $p185^{neu}$ and its derivatives could enhance transforming efficiency compared with cells expressing these mutant $p185^{neu}$ proteins alone. Cell lines listed in Table I (except kinase-deficient T691stop and Er/T691stop clones) were able to form foci independent of ligand stimulation (data not shown). Co-expression of EGFR with $p185^{neu}$ in Er/neu cells increased the ability to form foci, both in density and absolute number (by greater than 3-fold). However, co-expression of EGFR with kinase-active truncated mutant TAPstop or TΔ5 did not enhance focus formation efficiency in Er/TAPstop and Er/TΔ5 cells when compared with TAP/stop and TΔ5 cells, respectively (data not shown).

The colony growth efficiency of these clones in soft agar is also summarized in Table I. B104-1-1 cells expressing high levels of $p185^{neu}$ served as a positive control, while Er/T691stop clones served as a negative control and did not exhibit transformed colonies under the same conditions. Compared with B104-1-1 cells, cells expressing lower levels of oncogenic $p185^{neu}$ formed colonies less efficiently. However, more colonies were observed in EGFR-co-expressing Er/neu cells. Co-expression of EGFR with $p185^{neu}$ still permits functional heterodimerization in addition to homodimerization of either receptor, resulting in elevated biological activity, contributing to increased transforming activity *in vitro*. Cells expressing kinase-active truncated mutant TAPstop or TΔ5 mutant proteins alone displayed reduced colony growth efficiency in soft agar when compared with control B104-1-1 cells, although the expression levels of $p185^{neu}$ variants in these cells were similar. Critically, co-expression of EGFR with TΔ5 or TAPstop did not increase colony growth efficiency in soft agar.

Tumorigenicity was studied by injection of these mutant clones individually into athymic mice. Results are presented in Table I, which summarizes receptor expression levels, tumor frequency, and tumor size. B104-1-1 cells expressing oncogenic $p185^{neu}$ were used as a positive control and tumors caused by those cells appeared and grew quickly (with a latency of 5–7 days). No tumors were observed with kinase-deficient mutant clones T691stop and Er/T691stop cells (>10 weeks observation). Co-expression of EGFR and $p185^{neu}$, each at low levels, in Er/neu cells greatly accelerated tumor appearance (~2 weeks), and the tumors grew aggressively when compared with $p185^{neu}$ cells that also expressed low level of oncogenic $p185^{neu}$ (>4–5 weeks). Cooperative signaling between EGFR and $p185^{neu}$ was thus also observed in tumorigenicity assays *in vivo*. TΔ5 protein expression was sufficient to induce tumors (latency period of 2–3 weeks), and TAPstop mutant receptor expression also resulted in tumor formation (latency of 4–5 weeks). Receptor expression levels for these two mutant proteins was close to that in B104-1-1 cells. Notably, co-expression of EGFR with these mutant proteins, *i.e.* in Er/TAPstop and in Er/TΔ5, did not promote tumor growth.

The failure of distinct endodomain interactions between $p185^{neu}$ and EGFR, caused by an ectodomain deletion (TΔ5 mutant), or the lack of a functional COOH terminus (TAPstop mutant), clearly impairs signaling needed for transformation.

EGF-dependent Cell Proliferation of Cell Lines Co-expressing EGFR and Mutant $p185^{neu}$—To analyze whether EGF-dependent heterodimerization conveys signals leading to cooperative mitogenesis, we used the MTT assay to study proliferation of various cell lines. NE91 cells expressing EGFR only served as a positive control, and showed typical EGF induction of cell growth. As expected, the maximal induction dosage of EGF was 10 ng/ml, consistent with previous observations (44). However, the maximum induction dosage of EGF in Er/neu cells was ~0.1 ng/ml, 2 orders of magnitude less than that observed in NE91 cells (Fig. 5*A*). These data suggested that $p185^{neu}$ sensitized the EGF receptor responding to ligand.

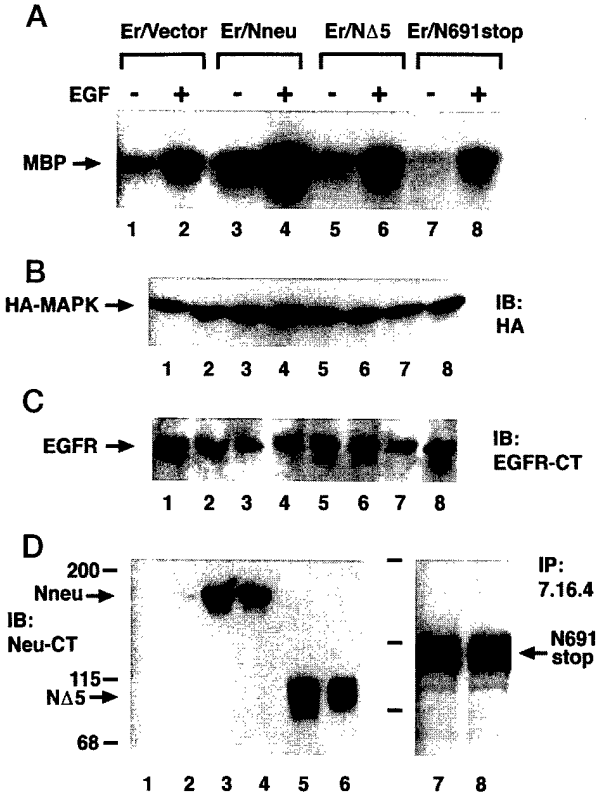

FIG. 6. **EGF-induced MAP kinase activity.** COS7 cells transiently expressing exogenous HA-MAPK, EGFR, and wild-type or mutant p185$^{c\text{-}neu}$ were treated with or without EGF (50 ng/ml) for 5 min as indicated. *A*, cells were then lysed, and anti-HA immunocomplexes were washed and underwent kinase reaction as described under "Experimental Procedures." The phosphorylation level of myelin basic protein were shown after autoradiography. *B–D*, equal amounts of cell extracts were used for examining ectopically expressed proteins. Antibodies used in immunoblot (*IB*) were indicated. Protein signals were developed by ECL. *Lanes 1–8* in these panels are correspondent to those in *panel A*. *D* (*lanes 7* and *8*), cells were metabolically labeled with [^{35}S]methionine and cell extracts were immunoprecipitated (*IP*) with 7.16.4 and analyzed in SDS-PAGE followed by autoradiography. Similar results were obtained in other two independent experiments.

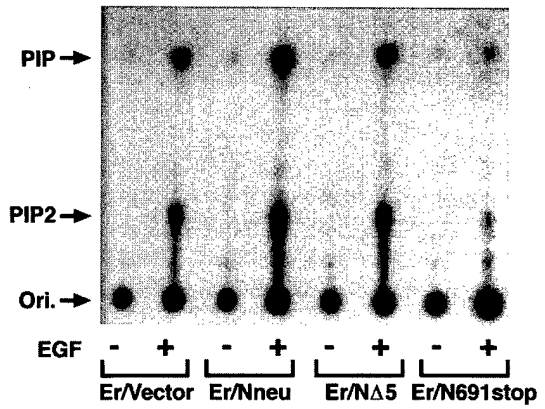

FIG. 7. **EGF-induced PI 3-kinase activity.** COS7 cells transiently expressing EGFR and wild-type or mutant p185$^{c\text{-}neu}$ (as indicated) were treated with or without EGF (50 ng/ml) for 5 min after serum starvation for 24 h. Equal amounts of cell extracts were immunoprecipitated by anti-Tyr(P) (4G10) and analyzed for PI 3-kinase activity as described under "Experimental Procedures." Autoradiogram of thin layer chromatography plate exposed overnight is shown. The positions of origin (*ori.*), phosphatidylinositol 3-phosphate (*PIP*), and phosphatidylinositol 3,4-bisphosphate (*PIP2*) were indicated by *arrows*. Data shown are representative of three individual experiments.

In contrast, the presence of T691stop in Er/T691stop cells suppressed the proliferative response to EGF, and cell growth was dramatically reduced (Fig. 5*B*). These results correlated with the inhibition of EGFR kinase (Figs. 3*E* and 4*B*). Interestingly, the EGFR in Er/TAPstop and Er/TΔ5 cells behaved normally in EGF-dependent mitogenesis when compared with that in NE91 cells, except that the basal growth level was higher (Fig. 5, *C* and *D*) due a more transformed phenotype (data not shown). These data correlated with previous observations (Figs. 2–4), suggesting that EGFR signaling is comparable in Er/TAPstop and in Er/TΔ5 clones to that seen in NE91 cells, *i.e.* neither enhanced nor suppressed. However, trans-receptor signaling was not observed due to either defective heterodimerization in Er/TAPstop cells or failure of heterodimerization in Er/TΔ5 cells.

EGF-dependent MAP Kinase and PI 3-Kinase Activation—To understand the mechanism underlying synergistic proliferative and transforming signal propagated by heteroreceptor interaction, we studied the EGF-induced MAP kinase and PI3 kinase pathways signaling phenomena. The proto-oncogenic p185 (Nneu) and its derivatives (NΔ5 or, N691stop) were co-expressed with EGFR, to evaluate EGF-dependent activation of downstream kinases, since p185^{neu} and TΔ5 are both constitutively active tyrosine kinases. An epitope-tagged HA-MAPK was also co-expressed with the combination of receptors in COS7 cells to examine downstream ERK activation.

Co-expression of p185$^{c\text{-}neu}$, but not NΔ5, with EGFR increased MAP kinase activity upon EGF stimulation. In contrast, EGFR-mediated MAP kinase activity in N691stop-co-expressing cells was suppressed when compared with cells expressing EGFR and an empty vector control (Fig. 6*A*). Equivalent protein expression levels of epitope-tagged HA-MAPK was also confirmed in these studies (Fig. 6*B*). Ectopically expressed EGFR and wild-type or mutant p185 forms were detected by immunoblot using anti-receptor specific antisera (Fig. 6, *C* and *D*). Since the intracellular domain-deleted N691stop could not be recognized by antiserum against the Nneu COOH terminus, the expression of N691stop was independently confirmed using metabolic labeled cell extracts followed by anti-neu immunoprecipitation (Fig. 6*D*, *lanes 7* and *8*).

Activation of PI-3-kinase requires phosphorylation of the Src homology 2-containing adapter p85 by receptor tyrosine kinases. Phosphatidylinositides are critical signaling intermediates and influence cell growth, differentiation, and adhesion (52). ErbB family members, notably ErbB-3, have been shown to associate with the p85 subunit of PI 3-kinase (53). To examine the influence of wild-type or mutant p185 on EGF-dependent activation of PI 3-kinase, plasmids expressing EGFR with vector or p185 variants were transiently expressed in COS7 cells. PI 3-kinase activity was examined in serum-starved cells with or without EGF stimulation. We observed a similar magnitude of the EGF-induced PI 3-kinase activity in cells expressing EGFR only or Er/NΔ5. The PI 3-kinase activity was much greater in Er/p185$^{c\text{-}neu}$ cells, and much weaker in Er/N691stop cells (Fig. 7). Expression patterns of these receptor proteins were determined (Fig. 6, *C* and *D*).

The observed super PI 3-kinase activity in Er/p185$^{c\text{-}neu}$ cells may arise through the tyrosine phosphorylation of the p85 subunit by the heteroreceptor complexes. We believe heteroreceptor complexes are more active since truncated p185 proteins alone do not seem effective at interaction with p85 (data not shown). Induced PI 3-kinase and MAPK activities therefore paralleled the heterodimerization and trans-activation events depicted in Figs. 2–4, and biological results obtained in Table I and Fig. 5. Functional heterodimerization observed in Er/neu cells permits cooperation and diversification of signaling, which contrasts with the formation of signaling-defective com-

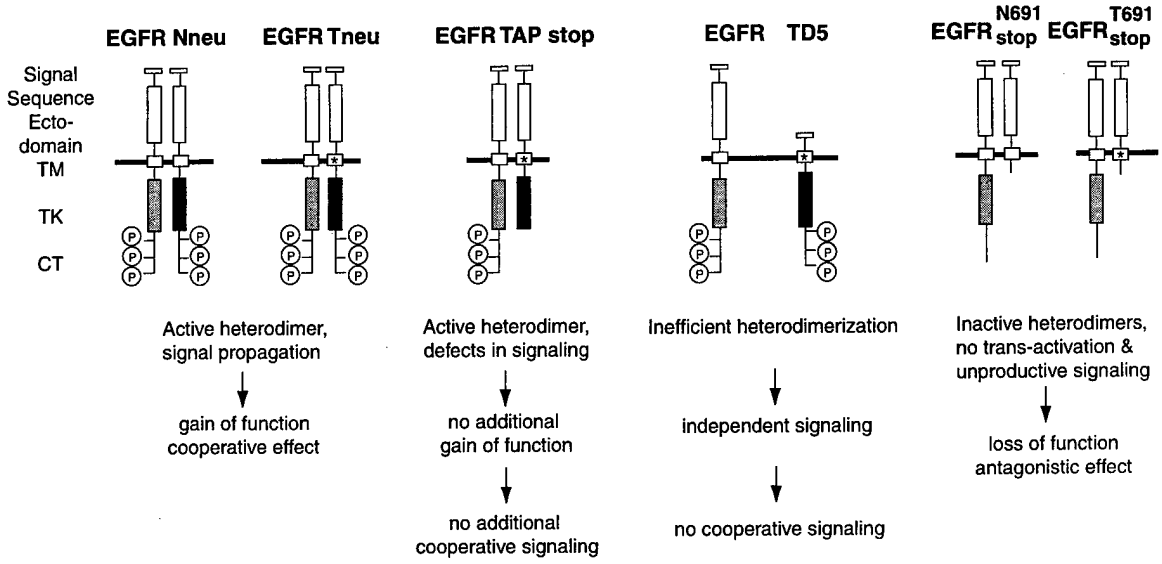

FIG. 8. **The role of p185^{neu} subdomains in heterodimerization with EGFR and resultant signaling consequences.** Functional heterodimerization requires the ectodomain for ligand-mediated physical associations, the endodomain for kinase transactivation, and the carboxyl terminus for cross-phosphorylation and combinatorial cellular signaling. Deletion of each subdomain results in inefficient heterodimerization, preventing kinase activation and defects in cooperative cellular signaling, respectively. *TD5*, TΔ5.

plexes in Er/T691stop cells or the failure of heterodimerization observed in Er/TΔ5 cells.

DISCUSSION

Using p185^{neu} mutants, which retain the capacity to homodimerize, we observed that EGF-induced heterodimerization could occur. Heterodimerization was seen in cells co-expressing EGFR with TAPstop or T691stop mutant receptors, but not with the extracellular domain-deleted TΔ5 (Fig. 2), demonstrating that the ectodomain of p185^{neu} is necessary and sufficient for heterodimerization with EGFR. Indeed, heterodimerization of the EGFR and N691stop form derived from proto-oncogenic p185^{neu} has been observed to occur preferentially to either p185$^{c\text{-}neu}$ or EGFR·EGFR homodimerization (37).

Two alternative assays confirmed trans-activation of ErbB family proteins following heterodimer formation. Anti-phosphotyrosine blotting showed that enhancement of tyrosine phosphorylation in response to EGF occurred only in cells co-expressing EGFR with the full-length p185^{neu} kinase, but not with the TAPstop or TΔ5 mutant receptors. It appears that EGFR and the T691stop neu mutant formed a kinase-inactive complex (Fig. 3), as described previously for the N691stop form (37).

An analysis of EGF-induced receptor internalization, a kinase-dependent event, also indicated that receptor trans-activation is required for efficient internalization of the EGFR found in these heteromers (Fig. 4). Full-length p185^{neu} and TAPstop proteins were modulated by EGF and showed co-internalization with EGFR efficiently, indicating an active heterodimer was formed. Co-expression of TΔ5 with EGFR did not affect normal endocytosis of EGFR since TΔ5 could not associate with EGFR, while T691stop neu expression interfered with normal EGFR down-modulation.

Recent studies have shown that the signal adapter Grb2 is required for efficient endocytosis of EGFR (54), and selective and regulated signal transduction from activated receptor tyrosine kinases may continue within the endosome (55). Interestingly, kinase-mediated activation of ERKs may also involve endocytotic trafficking since inhibition of clathrin-mediated endocytosis has been shown to impair rapid EGF-stimulated activation of ERKs (56). Therefore, it is reasonable to speculate that EGF-induced endocytosis of these receptor complexes reflects both heterodimeric kinase activity and the efficiency of activating downstream signaling components. Indeed, full-length p185^{neu}, but not other p185^{neu}-derived deletion mutants, displayed increased coupling of the Src homology 2-containing signaling molecule p85 to receptor activation (data not shown).

We previously reported that the co-expression of EGFR with p185$^{c\text{-}neu}$ (22), but not with kinase-deficient p185$^{c\text{-}neu}$ (44), synergistically transformed rodent fibroblasts. EGFR and p185$^{c\text{-}neu}$ associates into an active kinase complex (24) which upregulates EGF receptor function by increasing EGF binding affinity, ligand-induced DNA synthesis, and cell proliferation (23). In the current studies, when EGFR was co-expressed with oncogenic p185^{neu} at physiological levels (~10^4 receptors/cell), we also observed enhancement of tumor growth (4-fold) *in vivo* and anchorage-independent growth (~2-fold) *in vitro*, compared with the cells expressing p185^{neu} alone (Table I). Deletion of 122 amino acid residues from the carboxyl terminus of p185^{neu} eliminates three known tyrosine autophosphorylation sites (TAPstop mutant), and causes impaired cellular signaling and transforming potency (41). Overexpression of EGFR with the carboxyl-terminally truncated TAPstop mutant receptor, although leading to an active heterodimeric complex, did not recover the diminished transforming potency of TAPstop (Table I), indicating that signaling propagation through the carboxyl terminus of p185^{neu} could not be restored by association with full-length EGFR. These data emphasize that cooperative signaling requires not only the formation of an active kinase complex, but also a heteromeric functional carboxyl termini within the two receptor endodomains that recruit various downstream molecules required to generate signal to mediate cell growth and transformation.

The current results indicate that p185^{neu}·EGFR heterodimerization is greatly favored, even in the presence of the neu transmembrane point mutation that facilitates p185^{neu} homodimerization (12). Together with the observation that ErbB-2 is the preferred heterodimerization partner of all ErbB members (36), these studies emphasize that Neu·ErbB-2 may mediate signaling diversity through structural interactions governed by particular ectodomain sequences. For instance,

ErbB-3 is a less active kinase than other ErbB proteins (57), but serves as a binding site for Neu differentiating factor (28) and forms a potent heterodimer with ErbB-2, consequently engaging various downstream substrates. Neu·ErbB-2 may not be required for ligand binding, but may reconstitute signaling by laterally engaging other ErbB proteins in some preferred, but not well understood manner.

Kinase phosphorylation increases the affinity of binding of Src homology 2 and Src homology 3 domain-containing substrates, and initiates a variety of cascades. The binding of Grb2·Sos complexes to the active EGFR activates the Ras/Raf/MAP kinase cascade (58). Another downstream effector whose importance in cell signaling and, potentially, in tumorigenesis is becoming increasingly understood is PI 3-kinase (52). PI 3-kinase activation has also been shown to be essential for induction of DNA synthesis by EGF (59). Current studies have demonstrated that EGF-induced ErbB heterodimers activate both the ERK and PI 3-kinase pathways. Functional wild-type heterodimers, but not defective mutant heterodimers, efficiently induce both ERK and PI 3-kinase activities, which contribute to the synergistic effects on mitogenesis and cellular transformation.

As depicted in Fig. 8, these results further support the notion that cooperative signaling caused by $p185^{neu}$·EGF receptor ensembles requires the ectodomain for ligand-mediated physical association, while the intracellular domain provides contacts for efficient intermolecular kinase activation. The phosphorylated carboxyl terminus is essential for recruiting particular cellular substrates required for signal diversification.

In particular, specific ectodomain associations may therefore underlie the combinatorial interactions within the ErbB family required for signal diversification. These properties may be features that are used by many receptor ensembles involved in enzymatic signaling in cells.

REFERENCES

1. Ullrich, A., Coussens, L., Hayflick, J. S., Dull, T. J., Gray, A., Tam, A. W., Lee, J., Yarden, Y., Libermann, T. A., Schlessinger, J., Downward, J., Mayes, E. L. V., Whittle, N., Waterfield, M. D. & Seeburg, P. H. (1984) *Nature* **309,** 418–425
2. Schechter, A. L., Stern, D. F., Vaidyanathan, L., Decker, S. J., Drebin, J. A., Greene, M. I. & Weinberg, R. I. (1984) *Nature* **312,** 513–516
3. Yamamoto, T., Ikawa, S., Akiyama, T., Semba, K., Nomura, N., Miyajima, N., Saito, T. & Toyoshima, K. (1986) *Nature* **319,** 230–234
4. Kraus, M. H., Issing, W., Miki, T., Popescu, N. C. & Aaronson, S. A. (1989) *Proc. Natl. Acad. Sci. U. S. A.* **86,** 9193–9197
5. Plowman, G. D., Culouscou, J., Whitney, G. S., Green, J. M., Carlton, G. W., Foy, L., Neubauer, M. G. & Shonyab, M. (1993) *Proc. Natl. Acad. Sci. U. S. A.* **90,** 1746–1750
6. Dougall, W. C., Qian, X., Peterson, N. C., Miller, M. J., Samanta, A. & Greene, M. I. (1994) *Oncogene* **9,** 2109–2123
7. Lee, K. F., Simon, H., Chen, H., Hung, M. C. & Hauser, C. (1995) *Nature* **378,** 394–398
8. Gassmann, M., Casagranda, F., Orioli, D., Simon, H., Lai, C., Klein, R. & Lemke, G. (1995) *Nature* **378,** 390–394
9. Threadgill, D. W., Dlugose, A. A., Hansen, L. A., Tennenbaum, T., Lichti, U., Lee, D., LaMantia, C., Mourton, T., Herrup, K., Harris, R. C., Barnard, J. A., Yuspa, S. H., Coffey, R. J. & Magnuson, T. (1995) *Science* **269,** 230–234
10. O'Rourke, D. M., Zhang, X. & Greene, M. I. (1997) *Proc. Assoc. Am. Physicians* **109,** 209–219
11. Bargmann, C. I., Hung, M.-C. & Weinberg, R. A. (1986) *Cell* **45,** 649–657
12. Weiner, D. B., Liu, J., Cohen, J. A., Williams, W. V. & Greene, M. I. (1989) *Nature* **339,** 230–231
13. Weiner, D. B., Kokai, Y., Wada, T., Cohen, J. A., Williams, W. V. & Greene, M. I. (1989) *Oncogene* **4,** 1175–1183
14. Moscatello, D. K., Montgomery, R. B., Sundareshan, P., McDanel, H., Wong, M. Y. & Wong, A. J. (1996) *Oncogene* **13,** 85–96
15. O'Rourke, D. M., Nute, E. J. L., Davis, J. G., Wu, C., Lee, A., Murali, R., Zhang, H.-T., Qian, X., Kao, C.-C. & Greene, M. I. (1998) *Oncogene* **16,** 1197–1207
16. Slamon, D. J., Clark, G. M., Wong, S. G., Levin, W. J., Ullrich, A. & Mcguire, W. L. (1987) *Science* **235,** 177–182
17. Slamon, D. J., Godolphin, W., Jones, L. A., Holt, J. A., Wong, S. G., Kieth, D. E., Levin, W. J., Stuart, S. G., Udove, J., Ullrich, A. & Press, M. F. (1989) *Science* **244,** 707–712
18. Di Fiore, P. P., Pierce, J. A., Fleming, T. P., Hazan, R., Ullrich, A., King, C. R., Schlessinger, J. & Aaronson, S. A. (1987) *Cell* **51,** 1063–1070
19. Hudziak, R. M., Schlessinger, J. & Ullrich, A. (1987) *Proc. Natl. Acad. Sci. U. S. A.* **84,** 7159–7163
20. LeVea, C. M., Myers, J. N., Dougall, W. C., Qian, X. & Greene, M. I. (1993) *Receptor* **3,** 293–309
21. Samanta, A., LeVea, C. M., Dougall, W. C., Qian, X. & Greene, M. I. (1994) *Proc. Natl. Acad. Sci. U. S. A.* **91,** 1711–1715
22. Kokai, Y., Myers, J. N., Wada, T., Brown, V. I., LeVea, C. M., Davis, J. G., Dobashi, K. & Greene, M. I. (1989) *Cell* **58,** 287–292
23. Wada, T., Qian, X. & Greene, M. (1990) *Cell* **61,** 1339–1347
24. Qian, X. L., Decker, S. J. & Greene, M. I. (1992) *Proc. Natl. Acad. Sci. U. S. A.* **89,** 1330–1334
25. Goldman, R., Benlevy, R., Peles, E. & Yarden, Y. (1990) *Biochemistry* **29,** 11024–11028
26. Dougall, W. C., Qian, X., Miller, M. J. & Greene, M. I. (1996) *DNA Cell Biol.* **15,** 31–40
27. Qian, X., Dougll, W. C., Fei, Z. & Greene, M., I. (1995) *Oncogene* **10,** 211–219
28. Peles, E. & Yarden, Y. (1993) *BioEssays* **15,** 815–824
29. Carraway, K. L., III, Sliwkowski, M. X., Akita, R., Platko, J. V., Guy, P. M., Nuijens, A. A., Diamonti, J., Vandlen, R. L., Cantley, L. C. & Cerione, R. A. (1994) *J. Biol. Chem.* **269,** 14303–14306
30. Riese, D. J., van Raaij, T. M., Plowman, G. D., Andrews, G. C. & Stern, D. F. (1995) *Mol. Cell. Biol.* **15,** 5770–5776
31. Cohen, B. D., Green, J. M., Foy, L. & Fell, H. P. (1996) *J. Biol. Chem.* **271,** 4813–4818
32. Pinkas-Kramarski, R., Soussan, L., Waterman, H., Levkowitz, G., Alroy, I., Lavi, S., Seger, R., Ratzkin, B. J., Sela, M., & Yarden, Y. (1996) *EMBO J.* **15,** 2452–2467
33. Zhang, K., Sun, J., Liu, N., Wen, D., Chang, D., Thomason, A. & Yoshinaga, S. K. (1996) *J. Biol. Chem.* **271,** 3884–3890
34. Tzahar, E., Waterman, H., Chen, X., Levkowitz, G., Karunagaran, D., Lavi, S., Ratzkin, B. J. & Yarden, Y. (1996) *Mol. Cell. Biol.* **16,** 5276–5287
35. Alimandi, M., Romano, A., Curia, M. C., Muraro, R., Fedi, P., Aaronson, S. A., Di, F. P. & Kraus, M. H. (1995) *Oncogene* **10,** 1813–1821
36. Grause-Porta, D., Beerli, R. R., Daly, J. M. & Hynes, N. (1997) *EMBO J.* **16,** 1647–1655
37. Qian, X., Dougall, W. C., Hellman, M. E. & Greene, M. I. (1994)*Oncogene* **9,** 1507–1514
38. Drebin, J. A., Stern, D. F., Link, V. C., Weinberg, R. A. & Greene, M. I. (1984) *Nature* **312,** 545–548
39. Myers, J. N., LeVea, C. M., Smith, J. E., Kallen, R. G., Tung, L. & Greene, M. I. (1992) *Receptor* **2,** 1–16
40. Decker, S. J. & Harris, P. (1989) *J. Biol. Chem.* **264,** 9204–9209
41. Mikami, Y., Davis, J. G., Dobashi, K., Dougall, W. C., Myers, J. N., Brown, V. I. & Greene, M. I. (1992) *Proc. Natl. Acad. Sci. U. S. A.* **89,** 7335–7339
42. O'Rourke, D. M., Qian, X., Zhang, H. T., Davis, J. G., Nute, E., Meinkoth, J. & Greene, M. I. (1997) *Proc. Natl. Acad. Sci. U. S. A.* **94,** 3250–3255
43. Pruss, R. M. & Herschman, H. R. (1977) *Proc. Natl. Acad. Sci. U. S. A.* **74,** 3918–3921
44. Qian, X., LeVea, C. M., Freeman, J. K., Dougall, W. C. & Greene, M. T. (1994) *Proc. Natl. Acad. Sci. U. S. A.* **91,** 1500–1504
45. Moscatello, D. K., Holgado-Madrugal, M., Emlet, D. R., Montgomery, R. B. & Wong, A. J. (1998) *J. Biol. Chem.* **273,** 200–206
46. Stern, D. F. & Kamps, M. P. (1988) *EMBO J.* **7,** 995–1001
47. Akiyama, T., Saito, T., Ogawara, H., Toyoshima, K. & Yamamoto, T. (1988) *Mol. Cell. Biol.* **8,** 1019–1026
48. Kokai, Y., Dobashi, K., Weiner, D. B., Myers, J. N., Nowell, P. C. & Greene, M. I. (1988) *Proc. Natl. Acad. Sci. U. S. A.* **85,** 5389–5393
49. King, C. R., Borrello, I., Bellot, F., Comoglio, P. & Shlessinger, J. (1988) *EMBO J.* **7,** 1647–1651
50. Sorkin, A. & Waters, C. (1993) *BioEssays* **15,** 375–382
51. Segatto, O., Lonardo, F., Pierce, J. H., Bottaro, D. P. & Di Fiore, P. P. (1990) *New Biol.* **2,** 187–195
52. Hunter, T. (1997) *Cell* **88,** 333–346
53. Fedi, P., Pierce, L., Di Fiore, P. P. & Kraus, M. H. (1994) *Mol. Cell. Biol.* **14,** 492–500
54. Wang, Z. & Moran, M. F. (1996) *Science* **272,** 1935–1938
55. Bergeron, J. J., Di, G. G., Baass, P. C., Authier, F. & Posner, B. I. (1995) *Biosci. Rep.* **15,** 411–418
56. Vieira, A. V., Lamaze, C. & Schmid, S. L. (1996) *Science* **274,** 2086–2089
57. Guy, P., Platko, J. V., Cantley, L. C., Cerione, R. A. & Carraway, K. L. (1994) *Proc. Natl. Acad. Sci. U. S. A.* **91,** 8132–8136
58. Buday, L., and Downward, J. (1993) *Cell* **73,** 611–620
59. Roche, S., Koegl, M., and Courtneidge, S. A. (1994) *Proc. Natl. Acad. Sci. U. S. A.* **91,** 9185–9189

Proc. Natl. Acad. Sci. USA
Vol. 96, pp. 6434–6438, May 1999
Medical Sciences

Induction of the Tat-binding protein 1 gene accompanies the disabling of oncogenic erbB receptor tyrosine kinases

BYEONG-WOO PARK*, DONALD M. O'ROURKE*†, QIANG WANG*, JAMES G. DAVIS*, ANDREW POST*, XIAOLAN QIAN*, AND MARK I. GREENE*‡

Departments of *Pathology and Laboratory Medicine, and †Neurosurgery, Center for Receptor Biology and Cell Growth, University of Pennsylvania School of Medicine, 36th and Hamilton Walk, Philadelphia, PA 19104

Communicated by Peter C. Nowell, University of Pennsylvania School of Medicine, Philadelphia, PA, March 9, 1999 (received for review January 11, 1999)

ABSTRACT **Conversion of a malignant phenotype into a more normal one can be accomplished either by down-regulation of erbB family surface receptors or by creating inactive erbB heterodimers on the cell surface. In this report, we report the identification and cloning of differentially expressed genes from antibody-treated vs. untreated fibroblasts transformed by oncogenic p185^{neu}. We repeatedly isolated a 325-bp cDNA fragment that, as determined by Northern analysis, was expressed at higher levels in anti-p185^{neu}-treated tumor cells but not in cells expressing internalization defective p185^{neu} receptors. This cDNA fragment was identical in amino acid sequence to the recently cloned mouse Tat binding protein-1 (mTBP1), which has 98.4% homology to the HIV tat-binding protein-1 (TBP1). TBP1 mRNA levels were found to be elevated on inhibition of the oncogenic phenotype of transformed cells expressing erbB family receptors. TBP1 overexpression diminished cell proliferation, reduced the ability of the parental cells to form colonies *in vitro*, and almost completely inhibited transforming efficiency in athymic mice when stably expressed in human tumor cells containing erbB family receptors. Collectively, these results suggest that the attenuation of erbB receptor signaling seems to be associated with activation/induction or recovery of a functional tumor suppressor-like gene, *TBP1*. Disabling erbB tyrosine kinases by antibodies or by trans-inhibition represents an initial step in triggering a TBP1 pathway.**

ErbB family receptor kinases mediate oncogenic transformation by mutation, overexpression, or coexpression leading to homodimeric or heterodimeric complexes that mediate synergistic signaling (1–5). Continual expression of p185^{neu} is necessary for the maintenance of the neoplastic phenotype of neu-transformed cells (1). Incubation of oncogenic p185^{neu}-expressing tumor cells with the anti-neu mAb 7.16.4 causes phenotypic reversal *in vitro* and *in vivo* (6, 7). The mechanism of phenotypic reversal of tumor cells expressing the p185$^{neu/c\text{-}erbB2}$ oncogene occurring with anti-neu-specific mAb treatment has not been defined completely, although this mechanism has been characterized as arising as a consequence of disabling the kinase complex, a process in which a fraction of the receptors becomes down-modulated (6–8).

The binding of antibody to the extracellular domain of the p185^{neu} receptor mediates down-regulation and increases p185^{neu} oncoprotein degradation by causing the p185^{neu} complex to enter a degradation pathway. Endosomes were found to carry p185^{neu}-containing receptor aggregates to lysosomes where the complex was degraded (9).

Here, we used mRNA differential display (10, 11) to isolate genes that are specifically expressed in cells treated with the anti-p185^{neu} mAb 7.16.4. We repeatedly identified a 325-bp cDNA fragment called 3C bearing significant homology to the HIV tat-binding protein-1 (TBP1) on antibody-mediated down-regulation of the oncogenic p185^{neu} receptor associated with inhibition of transformation. The 3C fragment is completely identical to the recently cloned mouse tat binding protein-1 (mTBP1), which itself is 98% homologous to the human TBP1 over 439 aa (12). Northern blot analysis confirmed that this fragment and the TBP1 cDNA hybridized to mRNA isolated from cells undergoing phenotypic reversal by antibody treatment.

TBP1 has been reported to suppress tat-mediated transactivation of HIV replication (13). Nakamura *et al.* (12) established that full-length murine TBP1 also suppresses Tat-mediated transactivation. A TBP1-interacting protein (TBPIP), which colocalizes *in vivo* and synergistically enhances the inhibitory action of TBP1 on Tat activity *in vitro*, also has been cloned recently (14).

To investigate the biological effects of TBP1, we transfected the full length of TBP1 cDNA into a variety of human cell lines, U87MG, SK-BR-3, and MCF-7, which express erbB family genes. Ectopically expressed TBP1 was able to cause a reversion of the transformed phenotype. Additionally, basal TBP1 mRNA levels were found to be higher in phenotypically inhibited cells. These studies suggest that induction of TBP1 mediates inhibition of cell growth and transformation of erbB-inhibited cells.

MATERIALS AND METHODS

Cell Lines. B104-1-1 cells were derived from NIH 3T3 cells transfected with p185^{neu} and have been described (6). U87MG cells are human brain tumor cells; SK-BR-3 cells and MCF-7 cells are primary human breast cancer cells obtained from the American Type Culture Collection. These cells were cultured in DMEM containing 10% (vol/vol) FBS, 1% L-glutamine, and 1% penicillin/streptomycin at 37°C, 95% humidity, and 5% CO_2. The NR6TintΔ cells containing internalization-defective p185^{neu} receptors have been described (15).

Incubation of Cell Lines with mAb 7.16.4. The mAb 7.16.4 has been described (6, 7). B104-1-1 cells were grown overnight in 6-well dishes and treated with mAb 7.16.4 (10 μg/ml) for 0–4 h at 37°C. Cells were harvested, washed, stained with saturating amounts of mAb 7.16.4, and restained with anti-mouse IgG FITC. Cells were then processed for flow cytometric analysis as described (15).

RNA Isolation and mRNA Differential Display. Total RNA was purified from cell lysates by using the RNeasy Mini Kit (Qiagen, Valencia, CA) and the protocol supplied with the kit.

The publication costs of this article were defrayed in part by page charge payment. This article must therefore be hereby marked "*advertisement*" in accordance with 18 U.S.C. §1734 solely to indicate this fact.

PNAS is available online at www.pnas.org.

Abbreviations: RT-PCR, reverse transcriptase–PCR; MTT, 3-(4,5-dimethylthiazol-2-yl)-2,5-diphenyl tetrazolium bromide; EGFR, epidermal growth factor receptor.

‡To whom reprint requests should be addressed. e-mail: greene@reo.med.upenn.edu.

An mRNA Map Kit from GenHunter (Nashville, TN) was used, and the manufacturer's protocol was followed. DNase-treated total RNA (2 μg) was reverse-transcribed by using Super-Script II (United States Biochemical) with oligo(dT) primers T12MG, T12MC, or T12MA and amplified with the library 10-mers AP-3 (5′-AGGTGACCGT-3′) or AP-6 (5′-GCAATCGATG-3′) as described in the kit. The PCR products were run on a 6% sequence gel with the cDNAs that were to be compared run side-by-side. Bands representing differentially expressed genes were eluted from the gel, reamplified, subcloned into the pCRII vector as described in the TA cloning kit (Invitrogen), and sequenced on a 6% denaturing gel.

Generation of Stable TBP1 Transfectants and Confirmation of Transgene Expression by Reverse Transcriptase–PCR (RT-PCR). The TBP1 cDNA was inserted into the *Eco*RI site of the pBK-CMV (Stratagene) vector. Stable TBP1 transfectants were generated by transfecting the pBK-CMV–TBP1 plasmid into a panel of human cell lines (U87MG, SK-BR-3, and MCF-7) by using Lipofectamine (GIBCO). G418 (0.8 μg/ml; GIBCO) was used to select for the transfected cell populations, and Northern blot analysis was used to identify clones that expressed TBP1.

First-strand cDNA was prepared from 3 μg of total RNA by using the Superscript Preamplification System for first-strand cDNA Synthesis Kit (GIBCO/BRL). To confirm the integrity of the first-strand cDNAs, we amplified β-actin sequences by using the rat β-actin control amplifier set (CLONTECH), which yielded a 764-bp product. Exogenous/transfected TBP1-derived transcripts were amplified by using the pBK-CMV vector T7 primer (5′-GTAATACGCTCACTATAGGGC-3′) and a TBP1-specific primer designated C2 (5′-AGAAGAAAGCCAACCTAC-3′), which yielded a 216-bp product. After RT-PCR, the products were run on 1.8% agarose gels to evaluate the presence or absence of the amplified product.

Cell Proliferation Assay. The proliferation assay, as measured by 3-(4,5-dimethylthiazol-2-yl)-2,5-diphenyl tetrazolium bromide (MTT) incorporation, has been described (16).

***In Vitro* and *in Vivo* Tumorigenesis Assays.** Anchorage-independent growth was determined by assessing the colony-forming efficiency of cells suspended in soft agar (6, 17). For *in vivo* experiments, NCr homozygous nude mice (6–8 weeks old) were purchased from the National Cancer Institute (Bethesda, MD). Cells (1×10^6) were suspended in 0.1 ml of PBS and injected intradermally into the mid dorsum of each animal. Parental U87MG cells were injected on one side of individual animals and stably TBP1–cDNA-transfected U87/TBP1 cells were injected on the contralateral side to make direct comparisons of growth within each animal. Animals were maintained in accordance with guidelines of the Committee on Animals of the University of Pennsylvania and those of the Committee on Care and Use of Laboratory Animals of the Institute of Laboratory Animal Resources. Tumor growth was monitored twice weekly for 6–10 weeks. Tumor size was calculated by measuring tumor volume (length × width × thickness).

RESULTS

Down-Regulation of p185^{neu} Surface Receptors and Differentially Expressed Genes. Differential display provided a convenient way for us to study altered gene expression in p185^{neu}-expressing B104-1-1 murine cells treated with anti-p185^{neu}. One drawback of the differential display is its susceptibility to generating false–positive clones. To compensate, we ran two differential display trials on each of the total RNAs so that we could select bands that were present in both trials. There were nine differentially expressed bands chosen for further characterization; these bands ranged in size from 230 bp to 1,000 bp, were observed in both trials, and were not differentially expressed in NIH 3T3 cells. One of these bands represented a 325-bp cDNA termed 3C, which had 100% homology with mTBP1 (Fig. 1), which is the murine homologue of the human gene tat-binding protein 1. Northern blot analysis of 7.16.4-treated B104-1-1 cells showed increased TBP1 mRNA levels of ≈1.5 kb in size when probed by both human TBP1 cDNA (Fig. 2*A*) and 3C DNA (data not shown).

Confirmation of differential expression was achieved by comparing Northern blots of antibody-treated B104-1-1 cells and untreated cells (Fig. 2 *A* and *B*). Antibody treatment of B104-1-1 cells containing elevated levels of oncogenic p185^{neu} resulted in increased expression of the mTBP1 mRNA transcript (Fig. 2 *A* and *B*). We have shown that receptor kinase activity alone is not sufficient for the endocytic process (15). A structural element, namely an internalization sequence, is also required for both mAb- and ligand-induced receptor down-regulation (15). Importantly, NR6TintΔ cells (15), which contain an internalization-defective p185^{neu} mutant protein, TintΔ (15), and lack the ability to undergo p185^{neu} internalization, did not have an increase in mTBP1 mRNA level after 7.16.4 treatment, although the basal level of mTBP1 transcript was higher in NR6TintΔ cells (Fig. 2 *A* and *B*). Notably, B104-1-1 cells contain higher levels of transforming p185^{neu} than NR6TintΔ cells and are more oncogenic (15). The basal level of the mTBP1 transcript was, as expected, greater in the less oncogenic NR6TintΔ cell.

Because disabling erbB receptor ensembles may enable a common inhibitory pathway, we also examined cells in which EGFR was inactivated but not down-modulated by a trans-inhibitory ectodomain form of p185^{neu} (T691stop neu; refs. 17 and 18). We found that the endogenous expression of TBP1 mRNA was also higher in phenotypically inhibited U87MG-derived cells expressing the kinase-deficient T691stop neu ectodomain form compared with U87MG parental cells (Fig. 2*C*). Because T691stop inhibition of erbB kinase activity does not require erbB receptor down-modulation (17, 18), these data suggest that induction of TBP1 expression after anti-p185^{neu} mAb treatment occurs by regulation of a kinase signaling pathway (Fig. 2 *A* and *C*) and is not simply a result of receptor down-modulation and degradation (Fig. 2*C*).

Inhibition of Cell Growth and Transformation by Human TBP1. To investigate the biological effects of TBP1, we transfected, by using the pBK-CMV vector, full-length TBP1 cDNA into several different cell lines, SK-BR-3, MCF-7, and U87MG, all of which express erbB family receptors. We screened the transfected subclones by Northern blot analysis, and the expression of ectopic TBP1 in subclones was also confirmed by RT-PCR analysis (Fig. 3 *A* and *B*). We amplified a 216-bp product from all of the TBP1-cDNA-transfected clones and the pBK-CMV–TBP1 plasmid construct but not in the corresponding nontransfected parental cells (Fig. 3*A*). RT-PCR with a β-actin control amplifier set produced a 764-bp amplified product from all the cell lines except for the pBK-CMV–TBP1 plasmid construct (Fig. 3*B*).

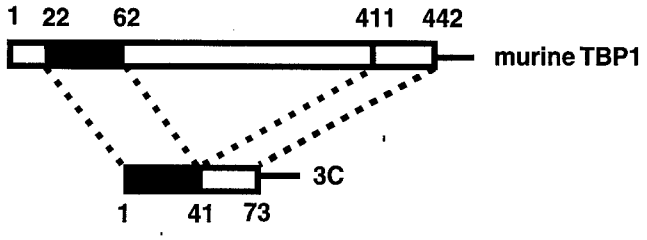

FIG. 1. Regions of homology of 3C to murine TBP1. Amino acids 1–41 of 3C correspond to amino acids 22–62 of mTBP1, and amino acids 42–73 of 3C correspond to amino acids 411–442 of mTBP1 (100% identical). The 3C C-terminal noncoding-region nucleotide sequence is 98% homologous to that of mTBP1.

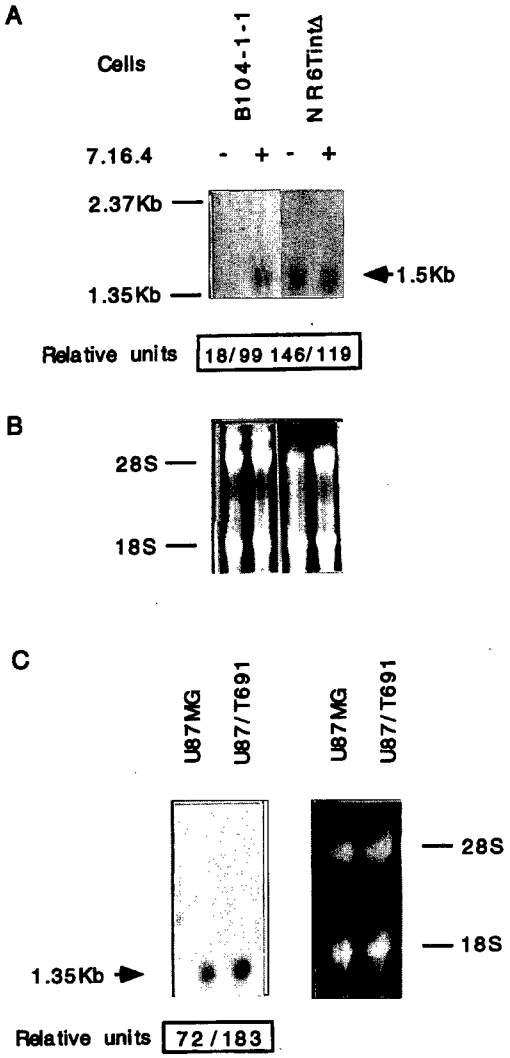

FIG. 2. Comparison and confirmation of the differentially expressed gene by Northern blot analysis and endogenous expression of TBP1 in U87MG vs. U87/T691. (*A*) B104-1-1 and NR6TintΔ cells were incubated with or without 7.16.4 (10 μg/ml) for 24 h before RNA isolation. Total RNA (10 μg) was loaded in each lane and was probed with human TBP1 cDNA probe. TBP1 expression was up-regulated with anti-p185^{neu} mAb (7.16.4) treatment in B104-1-1 cells (lanes 1 and 2) but was not changed in internalization defective NR6TintΔ cells (lanes 3 and 4). (*B*) The corresponding formaldehyde gel electrophoresis of total RNA is shown. (*C*) The U87/T691 subclone, an epidermal growth factor receptor (EGFR)-positive cell line phenotypically inhibited by the expression of a trans-inhibitory ectodomain form of p185^{neu} (T691 stop neu), showed increased endogenous levels of TBP1. Relative units are derived from scanning densitometry (Molecular Dynamics).

Cell growth of TBP1-transfected cells was evaluated by using the MTT assay (16). Transfected clones had 34–57% of proliferation inhibition compared with the corresponding parental cell lines (Fig. 4 *A–C*). Cell growth was therefore greatly diminished in TBP1-transfected erbB transformed cells. The level of TBP1 mRNA in the inhibited subclones was equal to, or exceeded, the amount of mRNA detected in parental cells inhibited by antibody treatment or T691stop expression. Thus, the mRNA level was sufficiently high to play a causal role in phenotypic reversion. Transformation efficiency was assessed by using an anchorage-independent growth assay (6, 17). The ability of TBP1 transfectants to form colonies was consistently and dramatically reduced (Fig. 5*A*). Transforming efficiency of SK-BR-3/TBP1, MCF-7/TBP1, and U87MG/TBP1 subclones was inhibited 79.2 ± 3.7% (mean ± SEM), 94.2 ± 4.5%, and

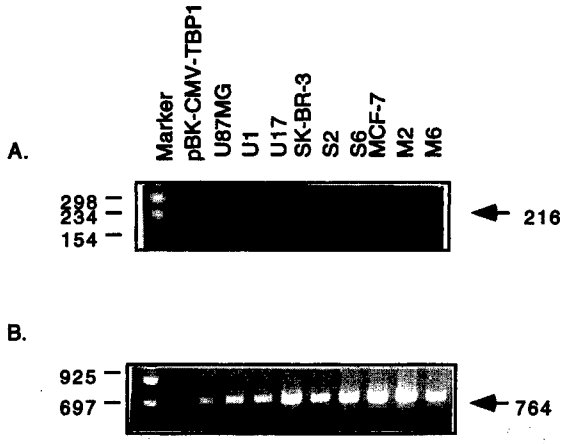

FIG. 3. Confirmation of TBP1-transfected clones by RT-PCR analysis. We made first-strand cDNA from 3 μg of each total RNA by using the Superscript Preamplification System for first-strand cDNA Synthesis Kit (GIBCO/BRL). (*A*) Amplification of the transfected TBP1 cDNA by using the pBK-CMV vector-oriented T7 primer (5′-GTAATACGCTCACTATAGGGC-3′) and the TBP1 specifically designed primer C2 (5′-AGAAGAAAGCCAACCTAC-3′) shows 216-bp product bands in only the transfected clones and the pBK-CMV–TBP1 plasmid construct and not in parental cell lines of U87MG, SK-BR-3, and MCF-7. (*B*) Amplification of actin cDNA by using the rat β-actin control amplifier set (CLONTECH) shows a 764-bp amplified product from all the cell lines except the pBK-CMV–TBP1 plasmid construct. After RT-PCR, the products were run on 1.8% agarose gel to confirm the amplified product.

65.5 ± 1.7%, respectively, as determined in three independent experiments. Transient transfection of U87MG cells with empty vector did not inhibit cell growth and transformation as determined by the MTT assay and by an anchorage-independent growth assay (data not shown).

U87/TBP1 subclones showed a profound degree of inhibition relative to U87MG parental cells after implantation into athymic mice (Fig. 5*B*). U87/TBP1 transfectants did not form appreciable tumors until 8 weeks (Fig. 5*B*), after the period of time when some animals injected with parental U87MG cells had to be killed because of excessive tumor burden. Additionally, more than 50% of the subcutaneous injections with the U87/TBP1 cell line failed to produce any palpable tumors.

DISCUSSION

Our findings indicate that disabling erbB oncoproteins with anti-erbB receptor antibodies leads to inhibition of the transformed phenotype, a feature associated with induction or recovery of TBP1 expression. Previous studies showed that kinase-deficient forms of p185^{neu} derived from the receptor ectodomain that form heterodimers with EGFR in rodent (19) and human glioblastoma cells can inhibit EGFR-dependent phenotypes contributing to transformation (17, 18). Endogenous expression of TBP1 mRNA is higher in U87MG human glioblastoma cells containing p185^{neu} kinase-deficient forms that have an inhibited phenotype. Although multiple TBP1 transfectants of three human cancer cell lines had an inhibited phenotype, all cell lines examined expressed erbB receptors. It remains possible that TBP1 induction accompanies reversion of transformation in non-erbB-containing cells. The degree to which TBP1 induction contributes to phenotypic reversion in erbB-inhibited cells is also unknown. Collectively, these observations suggest that expression of TBP1 is related to the tumorigenesis of certain malignant cells and that induction/recovery of TBP1 expression may be part of a general attenuating pathway or a specific consequence of down-regulation or attenuation of signaling from erbB family receptor tyrosine kinases.

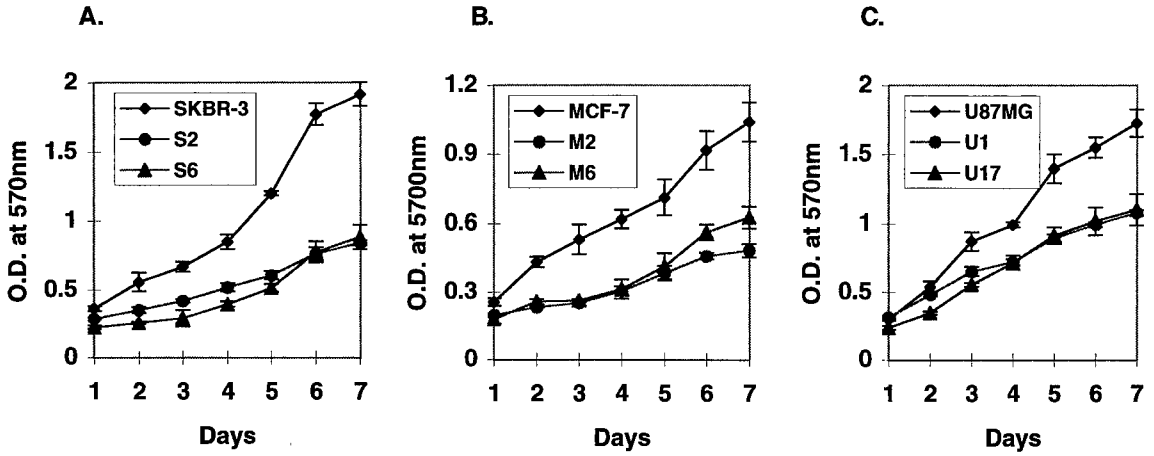

FIG. 4. Reduction of cell proliferation by expression of human TBP1 in human cancer cell lines. Cell lines were plated in 96-well plates at 4,000 cells per well in 10% DMEM and allowed to attach overnight. MTT was given to the cells for 4 h. Cells were then lysed in 50% (vol/vol) SDS/20% (vol/vol) dimethyl sulfoxide and kept at 37°C overnight. Proliferation was assessed by reading OD at 570 nm by using an ELISA reader. The number of cells used in this assay was determined to be within the linear range for this cell type. (*A*) TBP1 cDNA-transfected SK-BR-3 subclones S2 and S6 had 50% and 57% proliferation inhibition, respectively, compared with parental cells. (*B*) TBP1 cDNA-transfected MCF-7 subclones M2 and M6 had 40% and 54% proliferation inhibition, respectively, compared with parental cells. (*C*) U87MG subclones expressing elevated TBP1, U1, and U17 had 34% and 38% inhibition of proliferation, respectively, compared with parental cells.

The HIV tat protein, encoded by one of the viral regulatory genes, *tat*, is considered a powerful transactivator of viral gene expression (20–22). Human TBP1 is encoded by a 1,341-nt cDNA containing an ORF of 439 aa (23). TBP1 was originally described as a transcriptional factor of the HIV 1 by interaction with the tat protein (13, 23). TBP1 binds the HIV tat transactivator, suppressing its activity in cotransfection experiments (13). In some cases, TBP1 may also be involved in transcriptional activation (23). Nakamura *et al.* (12) isolated a full-length murine form of TBP1 that suppresses the Tat-mediated transactivation. Tanaka *et al.* (14) cloned a TBP1 interacting protein, TBPIP, that interacts with mTBP1. TBPIP colocalizes with TBP1 *in vivo* and synergistically enhances the inhibitory action of TBP1 on Tat activity *in vitro*, supporting the general concept of TBP1 ensembles that inhibit cellular functions and transcription.

We noted that TBP1 amino acids 59–63 bear 75% similarity to the motif HFRIG, and amino acids 185–189 bear 60% similarity to the motif HSRIG. The HIV gene *Vpr* contains a domain that contains two H(S/F)RIG motifs that may cause cell growth arrest and structural defects (24). *TBP1* also possesses 46% identity to *KAI1*, a metastasis suppressor gene for human prostate cancer (25). Hoyle *et al.* (26) recently localized the human *TBP1* to chromosome 11p12–13, and it has been noted that frequent loss of chromosome 11p13 occurs in a variety of cancers (27, 28). Tsuchiya *et al.* (29) reported that the tumor suppressor VHL gene product binds to TBP1. These observations suggest that the *TBP1* gene may be grouped with other possible functional tumor suppressor genes, and TBP1 may act as a negative regulator of the transcriptional elongation process by binding to tumor suppressor gene products such as pVHL.

All members of the TBP family, including TBP1, contain two highly conserved domains. One domain resembles a nucleotide-binding motif (ATP-binding site), and the other resembles a motif common to proteins with helicase activity. TBP1, TBP7, MSS1, and SUG1 are thus considered members of a large ATPase family rather than representing discrete transcriptional factors (30–33).

TBP1 has also been reported to be a component of the 26S proteasome (34), which is an essential multiprotein complex

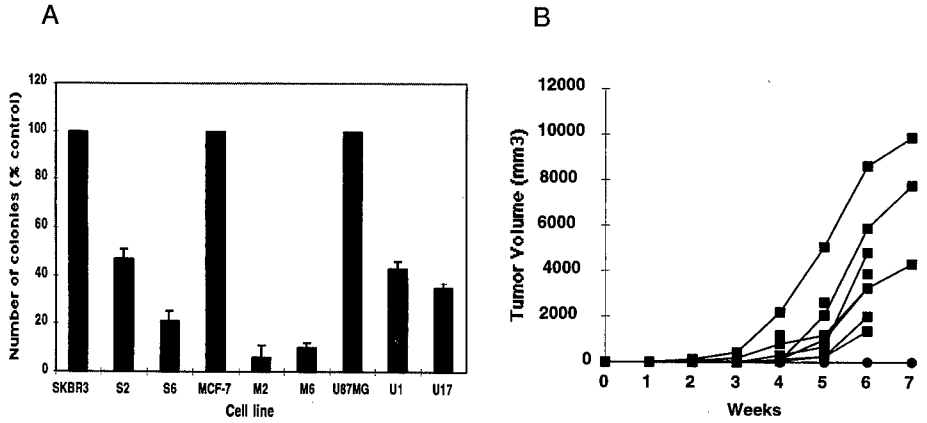

FIG. 5. Inhibition of cell growth and transformation by human TBP1. (*A*) Anchorage-independent growth. Cells of each clone (n = 1,000) were suspended in a 1-ml top layer [0.18% agarose/10% (vol/vol) FBS/10% (vol/vol) DMEM] in 6-cm culture dishes containing a 3-ml cell-free feeder layer consisting of 0.25% agarose in DMEM supplemented with 10% FBS and 20 mM Hepes (pH 7.5). Colonies (>0.3 mm) were visualized and counted on day 28 for all cell lines after staining with *p*-iodonitrotetrazolium violet (1 mg/ml). Each cell line was examined in triplicate in three separate experiments. The numbers of colonies reported represent the mean of triplicate samples. (*B*) Tumor growth in athymic mice: comparison of parental U87MG cells and U87/TBP1 transfectants. Cells of each cell line ($n = 1 \times 10^6$) were injected subcutaneously on day 0, and tumor volume was recorded weekly. These data represent individual tumor growth curves for U87MG parental cells (■) and mean tumor volumes for the U87/TBP1 subclone (●). (U87MG, n = 7; U87/TBP1, n = 8.)

that degrades ubiquitinated proteins in an ATP-dependent fashion and provides the main route for selective turnover of intracellular proteins involved with the regulation of cell growth and metabolism (35). TBP1 functions as a subunit of PA700, a nonproteasomal component of the 26S proteasome (34, 36), and a subunit of a proteasome modulator complex (34). Schnall *et al.* (37) isolated a set of 12 yeast genes, all belonging to the AAA family. Among them, the closest equivalents of the human genes *TBP1*, *TBP7*, and *MSS1* are named, respectively, *YTA1*, *YTA2*, and *YTA3*. These genes are identical or closely related to either cell cycle genes or to subunits of the 26S proteasome. We identified three proteins interacting with TBP1: p27 (34), p40 (38), and p42(SUG-2) (34, 39) in a yeast two-hybrid system by using a HeLa cell cDNA library (data not shown). Interestingly, p27 and p42 are subunits of the human proteasome 26S modulator complex, and both p40 and p42 are subunits of the regulatory proteasome PA 700. TBP1 itself is also a subunit of both the PA700 and modulator complex that enhances 26S proteasome activity (34). Moreover, DeMartino *et al.* (34) reported the purification and characterization of a proteasomal modulator complex—a trimer of TBP1, p42, and p27—which enhances proteasomal activity by as much as 8-fold. Recently, Watanabe *et al.* (40) established the association of p27, p42, and TBP1 with not only the modulator complex but also with the 26S proteasome complex. High sequence similarities of TBP1 homologues over widely different species substantiate that TBP1 function is essential *in vivo* (12). These results suggest a relationship between TBP1 expression and a protein degradation pathway.

Cell surface levels of $p185^{neu}$ and EGFR were independently down-regulated on expression of TBP1 in all subclones examined by flow cytometric analysis (B.-W.P. and M.I.G., unpublished results). These results suggest that TBP1 activity is related to inactivation of surface $p185^{neu}$ and EGFR. TBP1, as a human 26S proteasome modulator (34), may increase proteasomal activity by facilitating degradation of sequestered cell-surface proteins in addition to its role in transcriptional regulation.

This study shows that TBP1 expression was up-regulated with anti-$p185^{neu}$ mAb (7.16.4) treatment in B104-1-1 cells but not in NR6TintΔ cells expressing internalization-defective $p185^{neu}$ proteins (Fig. 2*A*). U87/T691 cells, an EGFR-disabled cell line containing a trans-inhibitory ectodomain form of $p185^{neu}$ (T691stop neu), also showed an increased endogenous level of TBP1 over that observed in parental U87MG cells (Fig. 2*C*). Our findings suggest that TBP1 expression is inversely related to the "activity" of the kinase signaling pathway (Fig. 2 *A* and *C*) and is not necessarily a direct result of the receptor degradation alone (Fig. 2*C*). Attenuation of erbB receptor signaling seems to involve the activation of a functional tumor suppressor-like gene, *TBP1*, which itself is associated with a proteasomal protein degradation pathway.

1. Dougall, W. C., Qian, X., Peterson, N. C., Miller, M. J., Samanta, A. & Greene, M. I. (1994) *Oncogene* **9,** 2109–2123.
2. Kiyokawa, N., Yan, D. H., Brown, M. E. & Hung, M. C. (1995) *Proc. Natl. Acad. Sci. USA* **92,** 1092–1096.
3. Wada, T., Qian, X. L. & Greene, M. I. (1990) *Cell* **61,** 1339–1347.
4. Alimandi, M., Romano, A., Curia, M. C., Muraro, R., Fedi, P., Aaronson, S. A., DiFiore, P. P. & Kraus, M. H. (1995) *Oncogene* **10,** 1813–1821.
5. Pinkas-Kramarski, R., Soussan, L., Waterman, H., Levkowitz, G., Alroy, I., Klapper, L., Lavi, S., Seger, R., Ratzkin, B. J., Sela, M., *et al.* (1996) *EMBO J.* **15,** 2452–2467.
6. Drebin, J. A., Link, V. C., Stern, D. F., Weinberg, R. A. & Greene, M. I. (1985) *Cell* **41,** 695–706.
7. Drebin, J. A., Link, V. C., Weinberg, R. A. & Greene, M. I. (1986) *Proc. Natl. Acad. Sci. USA* **83,** 9129–9133.
8. Katsumata, M., Okudaira, T., Samanta, A., Clark, D. P., Drebin, J. A., Jolicoeur, P. & Greene, M. I. (1995) *Nat. Med.* **1,** 644–648.
9. Brown, V. I., Shan, N., Smith, R., Hellman, M., Jarett, L., Mikami, Y., Cohen, E., Qian, X. & Greene, M. I. (1994) *DNA Cell Biol.* **13,** 193–209.
10. Liang, P. & Pardee, A. B. (1992) *Science* **257,** 967–971.
11. Liang, P., Averboukh, L. & Pardee, A. B. (1993) *Nucleic Acids Res.* **21,** 3269–3275.
12. Nakamura, T., Tanaka, T., Takagi, H. & Sato, M. (1998) *Biochim. Biophys. Acta* **1399,** 93–100.
13. Nelbock, P., Dillon, P. J., Perkins, A. & Rosen, C. A. (1990) *Science* **248,** 1650–1653.
14. Tanaka, T., Nakamura, T., Takagi, H. & Sato, M. (1997) *Biochem. Biophys. Res. Commun.* **239,** 176–181.
15. Qian, X., O'Rourke, D. M., Drebin, J., Zhao, H., Wang, Q. & Greene, M. I. (1997) *DNA Cell Biol.* **16,** 1395–1405.
16. Hansen, M. B., Nielsen, S. E. & Berg, K. (1989) *J. Immunol. Methods* **119,** 203–210.
17. O'Rourke, D. M., Qian, X., Zhang, H.-T., Davis, J. G., Nute, E., Meinkoth, J. & Greene, M. I. (1997) *Proc. Natl. Acad. Sci. USA* **94,** 3250–3255.
18. O'Rourke, D. M., Nute, E. J. L., Davis, J. G., Wu, C., Lee, A., Muralli, R., Zhang, H.-T., Qian, X., Kao, C.-C. & Greene, M. I. (1998) *Oncogene* **16,** 1197–1207.
19. Qian, X., O'Rourke, D. M., Zhao, H. & Greene, M. I. (1996) *Oncogene* **13,** 2149–2157.
20. Sodroski, J., Patarca, R., Rosen, C., Wong-Staal, F. & Haseltine, W. (1985) *Science* **229,** 74–77.
21. Sodroski, J., Goh, W. C., Rosen, C., Dayton, A., Terwilliger, E. & Haseltine, W. (1986) *Nature (London)* **321,** 412–417.
22. Feinberg, M. B., Jarrett, R. F., Aldovini, A., Gallo, R. C. & Wong-Staal, F. (1986) *Cell* **46,** 807–817.
23. Ohana, B., Moore, P. A., Ruben, S. M., Southgate, C. D., Green, M. R. & Rosen, C. A. (1993) *Proc. Natl. Acad. Sci. USA* **90,** 138–142.
24. Macreadie, I. G., Castelli, L. A., Hewish, D. R., Kirkpatrick, A., Ward, A. C. & Azad, A. A. (1995) *Proc. Natl. Acad. Sci. USA* **92,** 2770–2774.
25. Dong, J. T., Lamb, P. W., Rinker-Schaeffer, C. W., Vukanovic, J., Ichikawa, T., Isaacs, J. T. & Barrett, J. C. (1995) *Science* **268,** 884–886.
26. Hoyle, J., Tan, K. H. & Fisher, E. M. (1997) *Hum. Genet.* **99,** 285–288.
27. Bepler, G. & Garcia-Blanco, M. A. (1994) *Proc. Natl. Acad. Sci. USA* **91,** 5513–5517.
28. Shipman, R., Schraml, P., Colombi, M., Raefle, G. & Ludwig, C. U. (1993) *Hum. Genet.* **91,** 455–458.
29. Tsuchiya, H., Iseda, T. & Hino, O. (1996) *Cancer Res.* **56,** 2881–2885.
30. Dubiel, W., Ferrell, K., Pratt, G. & Rechsteiner, M. (1992) *J. Biol. Chem.* **267,** 22699–22702.
31. Dubiel, W., Ferrell, K. & Rechsteiner, M. (1994) *Biol. Chem. Hoppe-Seyler* **375,** 237–240.
32. Leeb, T., Rettenberger, G., Breech, J., Hameister, H. & Brenig, B. (1996) *Mamm. Genome* **7,** 180–185.
33. Swaffield, J. C., Melcher, K. & Johnston, S. A. (1995) *Nature (London)* **374,** 88–91.
34. DeMartino, G. N., Proske, R. J., Moomaw, C. R., Strong, A. A., Song, X., Hisamatsu, H., Tanaka, K. & Slaughter, C. A. (1996) *J. Biol. Chem.* **271,** 3112–3118.
35. Ciechanover, A. (1994) *Cell* **79,** 13–21.
36. Kominami, K., DeMartino, G. N., Moomaw, C. R., Slaughter, C. A., Shimbara, N., Fujimuro, M., Yokosawa, H., Hisamatsu, H., Tanahashi, N., Shimizu, Y., *et al.* (1995) *EMBO J.* **14,** 3105–3115.
37. Schnall, R., Mannhaupt, G., Stucka, R., Tauer, R., Ehnle, S., Schwarzlose, C., Vetter, I. & Feldmann, H. (1994) *Yeast* **10,** 1141–1155.
38. Tsurumi, C., DeMartino, G. N., Slaughter, C. A., Shimbara, N. & Tanaka, K. (1995) *Biochem. Biophys. Res. Commun.* **210,** 600–608.
39. Bauer, V. W., Swaffield, J. C., Johnston, S. A. & Andrews, M. T. (1996) *Gene* **181,** 63–69.
40. Watanabe, T. K., Saito, A., Suzuki, M., Fujiwara, T., Takahashi, E., Slaughter, C. A., DeMartino, G. N., Hendil, K. B., Chung, C. H., Tanahashi, N., *et al.* (1998) *Genomics* **50,** 241–250.